UNIVERSITÀ
DEGLI STUDI
DI PADOVA

Sede Amministrativa: Università degli Studi di Padova

Dipartimento di Medicina Molecolare

CORSO DI DOTTORATO DI RICERCA IN: MEDICINA MOLECOLARE
CURRICULUM: BIOMEDICINA
CICLO XXXIV

Exploring the link between Metabolism and Ferroptosis: a focus on Pyruvate Dehydrogenase Complex

Coordinatore: Ch.mo Prof. Riccardo Manganelli
Supervisore: Ch.mo Prof. Fulvio Ursini
Co-Supervisore: Ch.ma Dott.ssa Valentina Bosello Travain

Dottorando : Elena Tibaldi

ABSTRACT

Ferroptosis is a form of regulated cell death operated by iron-dependent lipid peroxidation. Ferroptosis is primed by the missing or insufficient activity of the Glutathione Seleno-Peroxidase 4 (GPx4), which catalyzes the glutathione (GSH)-dependent reduction of lipid hydroperoxides to the corresponding alcohols. Besides GPx4 inactivation, ferroptosis occurs when other conditions are satisfied: -oxygen metabolism leading to the continuous formation of traces of LOOH from phospholipid-containing polyunsaturated fatty acids; - availability of ferrous iron from the labile iron pool. Consistently with the critical role of the traces of LOOH, we recently proposed that ferroptosis follows the loss of homeostatic control between the oxidative challenge posed by aerobic metabolism and GPx4 activity. The working hypothesis, supported by acknowledged chemical mechanisms, was that $O_2^{\bullet-}$ arising from aerobic metabolism accounts for the formation of the tiny amounts of LOOH sparking iron-dependent LPO and thus ferroptosis.

This work aimed to shed light on the relationship between aerobic mitochondrial metabolism and ferroptosis induced by GSH depletion, focusing on the site of production and the mechanism of reactions leading to the indispensable formation of traces amounts PL-OOH from which iron initiates LPO when GPx4 activity is insufficient.

In our cell model, we failed to detect a role of respiratory chain. We observed instead that the pyruvate dehydrogenase complex supports ferroptosis. By silencing either the E1 or the E3 subunit of the pyruvate dehydrogenase complex, the autoxidation of dihydrolipoamide emerges as the source of superoxide. In this respect, we observed that GSH depletion activates superoxide production, through the inhibition of the specific kinase that inhibits pyruvate dehydrogenase. Finally, we observed the contribution of autophagy in mediating ferroptosis due to GSH depletion.

RIASSUNTO

La ferroptosi è una forma di morte cellulare regolata, dovuta alla perossidazione lipidica dipendente dal ferro. La ferroptosi viene innescata dalla mancata attività dell'enzima glutathione perossidasi 4 (GPx4), che catalizza la riduzione glutatione (GSH)-dipendente degli idroperossidi di membrana ad alcoli corrispondenti. Oltre all'inattivazione di GPx4, la ferroptosi avviene quando sono soddisfatte altre condizioni: -la presenza del metabolismo aerobico che porta alla continua formazione di tracce di idroperossidi a partire dai fosfolipidi contenenti acidi grassi polinsaturi; - la disponibilità di ferro ridotto dal pool labile di ferro. In accordo con il ruolo critico delle tracce di LOOH, di recente abbiamo proposto che la ferroptosi possa essere dovuta alla perdita del controllo omeostatico tra l'ambiente ossidativo dovuto al metabolismo aerobico e l'attività di GPx4. L'ipotesi di lavoro è che $O_2^{\bullet-}$ derivante dal metabolismo aerobico sia responsabile delle tracce di LOOH che iniziano la perossidazione lipidica e di conseguenza la ferroptosi. Questo lavoro è stato volto alla ricerca della relazione tra metabolismo aerobico mitocondriale e ferroptosi dovuta a deplezione di GSH, con un focus sul sito di produzione ed il meccanismo reazione che porta alla formazione di tracce di PL-OOH dalle quali il ferro innesca la perossidazione lipidica se l'attività di GPx4 è insufficiente. Nel nostro modello, non abbiamo rilevato il coinvolgimento della catena respiratoria ma abbiamo osservato chela piruvato deidrogenasi sostiene la ferroptosi. Silenziando alternativamente la subunità E1 o E3 abbiamo stabilito che la fonte dell'anione superossido è data dall'autossidazione della diidrolipoamide. A questo riguardo, abbiamo osservato che la deplezione di GSH attiva la produzoine di anione superossido attraverso l'inibizione della chinasi (PDK) che inibisce la piruvato deidrogenasi. Infine abbiamo dimostrato che l'autofagia svolge un ruolo nel mediare la ferroptosi dovuta a deplezione di GPx4.

Sommario

INTRODUCTION 7

1.1 Cell Death 7

1.2 Ferroptosis 8

1.2.1 Molecular mechanism of ferroptosis 10

1.2.2 Positive regulators of Ferroptosis 11

1.2.2.1.Lipid peroxidation 11

1.2.2.2 Iron 15

1.2.3 Negative regulators of Ferroptosis 16

1.2.3.1 PIP, PHGPx, GPx4 16

1.2.3.1.1 GPx4 structure 16

1.2.3.1.2 GPx4 kinetics and catalytic mechanism 17

1.2.3.2 GSH 19

1.2.3.3 FSP1, a GSH-independent inhibitor of ferroptosis 20

1.2.4 Contribution of metabolism to Ferroptosis 21

1.2.5 Relevance of ferroptosis in physiological and pathological conditions 22

AIM 23

MATERIAL AND METHODS 24

3.1. Cell culture and reagents 24

3.2. Cell viability assay 24

3.3. Measurement of total GSH 24

3.4. Measurement of the oxygen consumption rate 25

3.5. Measurement of C11 bodipy oxidation 25

3.6. mRNA silencing 25

3.7 qRT-PCR mRNA quantification 26

3.8. Western blotting 26

3.9. Mitochondrial $O^{2\cdot-}$ determination 27

3.10. Statistical analysis 27

RESULTS 28

4.1 Cell density regulates sensitivity to ferroptosis 28

4.2. The mitochondrial respiratory chain is not involved in Ferroptosis 29

4.3 Role of the energetic substrates in erastin-induced ferroptosis 30

4.4 Role of Pyruvate Dehydrogenase Complex (PDC) 31

4.5 Role of Pyruvate Dehydrogenase kinase 35

4.6 Mechanism of GPx4 inactivation by GSH depletion in HT1080 cells 36

CONCLUSIONS 38
REFERENCES 40

INTRODUCTION

1.1 Cell Death

As defined by the Nomenclature Committee on Cell Death (NCCD) “cell death is the irreversible degeneration of vital cellular functions, ATP production and preservation of redox homeostasis, culminating in the loss of cellular integrity intended as plasma membrane permeabilization or cellular fragmentation”. This may be the result of the natural process of old cells dying and being replaced by new ones, or may result from disease, localized injury, or other environmental agents [1].

Cell death is a process defined by specific mechanisms shared by all organisms. The classifications of them started since it was first described, and was based upon differences in morphological features accompanying dying cell and divided cell death in: i) apoptosis (type I) characterized by chromatin condensation and nuclear fragmentation of cells undergoing phagocytosis, ii) autophagy (type II), exhibiting cytoplasmatic vacuolization in dying cells, similarly activating phagocytosis and lysosomal degradation; iii) and necrosis (type III), associated with fragmentation without phagocytic and lysosomal involvement [1, 2].

According to the latest recommendations of the NCCD in 2018, there are currently two types of cell death, defined as accidental cell death (ACD) and regulated cell death (RCD) [1]. Accidental cell death is an unexpected uncontrolled process due to chemical, physical, or mechanical issues, whereas RCD is based on a tightly controlled molecular machinery, implying that it can be pharmacologically or genetically regulated. RCD accounts for cell death that occurs in two different opposite situations: i) in absence of an external environmental alteration, due to a physiological program of tissue development, remodelling as well as cell turnover; ii) in presence of such perturbations, regarding intracellular and/or extracellular microenvironment, to which cell cannot counteract. [2].

RCD is further divided into apoptotic and nonapoptotic forms (e.g., ferroptosis, necroptosis, pyroptosis, and alkaliptosis), which have different characteristics of signal induction and molecular modulation as well as disease implications [3].

As research continues and novel signalling pathways governing RCD are still being characterized, the last updated classification of cell death modalities considers the molecular aspects of the process, in particular the signal transduction pathways responsible of initiation,

execution, and propagation of cell death, together with the physiological and pathological importance of each types of RCD. The complexity of new classification is well depicted in Figure 1 [1].

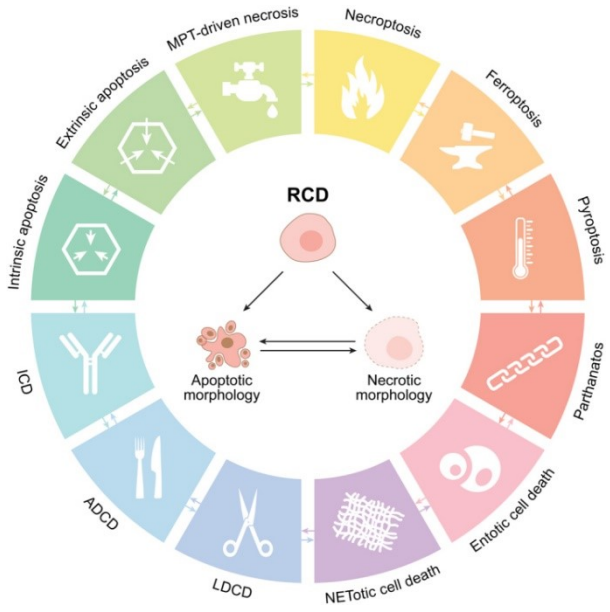

Figure 1. Major cell death subtypes, adapted from [1]. ADCD: autophagy-dependent cell death, ICD: immunogenic cell death, LDCD: lysosome-dependent cell death, MPT: mitochondrial permeability transition.

In such a dynamic and fascinating scenario, I focused my attention on ferroptosis, which best underlines the concept of redox homeostasis , and best describes the dual role of oxygen, at the same time supporting life and death.

1.2 Ferroptosis

Ferroptosis is a newly described form of regulated cell death, initiated by oxidative perturbations of the intracellular microenvironment sparked by missing or insufficient activity of the selenoperoxidase Glutathione Peroxidase 4 (GPx4), causing the specific form of cell death operated by membrane lipid peroxidation (LPO) [5]. The first description of lipid peroxidation of biological membranes was proposed more than 60 years ago, but only in the last few years these reactions started being considered as they are: biologically regulated events impacting on cell life and death [6].

Nowadays ferroptosis is regarded as one of the most common and ancient forms of cell death: although originally studied in mammalian cells, "Ferroptosis-like" cell death has also been noted in evolutionarily remote species, belonging to the kingdoms of plants, protozoa and fungi [7].

Lipid peroxidation emerged as the executor of ferroptosis from studies using lethal molecules depleting the substrate of GPx4, glutathione (GSH), or directly inhibiting GPx4 [4,8]. GPx4 negatively regulates ferroptosis by reducing phospholipid hydroperoxides (PL-OOH) into corresponding alcohols (PL-OH) using two molecules of GSH [9]. Therefore, ferroptosis only occurs when GPx4 cannot deal with PL-OOH normally produced by cellular processes. Thus, it is clear that ferroptosis is not the endpoint of a cellular pathway initiated by a specific agonist, as it happens for apoptosis, but it is the result of insufficient enzymatic control of lipid peroxidation.

Lipid peroxidation plays a central role since integrates multiple environmental and genetic signals, including redox homeostasis, metabolism, oncogenic and oncosuppressor signalling [7].

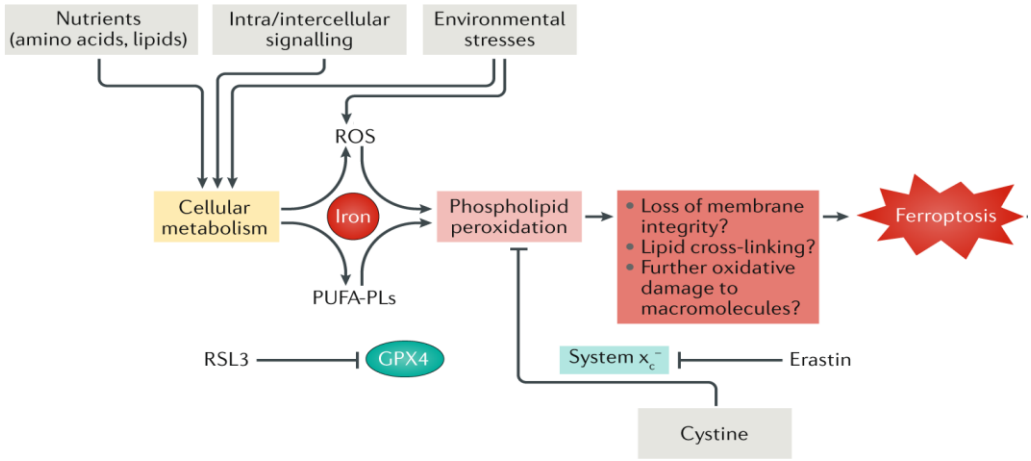

Figure 2. An overview on Ferroptosis, adapted from [7]. See text for details.

Originally, the term ferroptosis described the peculiar features of cell death induced by either RAS selective lethal 3 (RSL3) molecule or a small molecule erastin, discovered in synthetic lethal screening using small molecule libraries [8, 10]. Stockwell et al. observed that those two compounds were able to induce cell death in cells expressing oncogenic mutant HRAS and T oncoproteins with different unknown modality. In contrast to other forms of cell death, ferroptotic cells appeared rounded and detached, with aberrant mitochondrial morphology [4].

In this respect, mitochondria lose structural integrity accompanied by increased mitochondrial membrane density and loss of cristae, as revealed by electron microscopy [11]. Contrary to apoptosis, nucleus morphology didn't change and no chromatin condensation was observed. Furthermore these cell displayed a strong correlation with cellular iron content and availability . Indeed, ferroptosis is prevented by strong iron chelators. This concept associated to the protective effect of iron chelators and lipophilic antioxidants contributed to the definition of ferroptosis as a form of RCD operated by lipid peroxidation.

1.2.1 Molecular mechanism of ferroptosis

Starting from Stockwell findings, in the following years, some mechanistic details of Ferroptosis have been discovered by using different classes of Ferroptosis inducing agents (FINs). The inhibition of cystine (Cys-S-S-Cys) uptake via the cystine/glutamate antiporter Xc- represents an indirect mechanism of induction of ferroptosis. System Xc- is a heterodimeric protein complex, located in the plasma membrane, composed of a channel protein, namely SLC7A11 (xCT), linked to the regulatory protein SLC3A2 (4f2hc) by a disulfide bridge [12]. Although the flow is possible in both directions, in normal experimental conditions Xc- antiporter allows the import of extracellular cystine with concomitant export of intracellular glutamate (Glu). Cystine inside the cell is reduced by GSH or thioredoxin reductase 1 (TXNRD1) to cysteine (Cys) and used for GSH synthesis [13]. GSH is a tripeptide consisting of Glu, Cys and glycine (Gly) and is synthetized in two ATP dependent reactions: first, the enzyme γ-glutamylcysteine ligase (GCL) catalyses the formation of γ-glutamylcysteine from Glu and Cys, and this is the rate-limiting step of GSH synthesis; second, glutathione synthetase (GS) adds Gly to γ-glutamylcysteine forming γ-glutamyl-cysteinyl-glycine.

GSH is substrate of both oxidoreductases and transferases as a nucleophilic molecule. In details, in the case of GPx4, GSH is the nucleophilic substrate for the reaction of membrane lipid hydroperoxide reduction.

System Xc- inhibition with small molecules such as erastin, and sorafenib or direct inhibition with buthionine sulfoximine (BSO) and derivatives, act by causing a drop in GSH content and subsequently a reduction of GPx4 activity and finally membrane lipid peroxidation executing ferroptotic cell death [4,14,15].

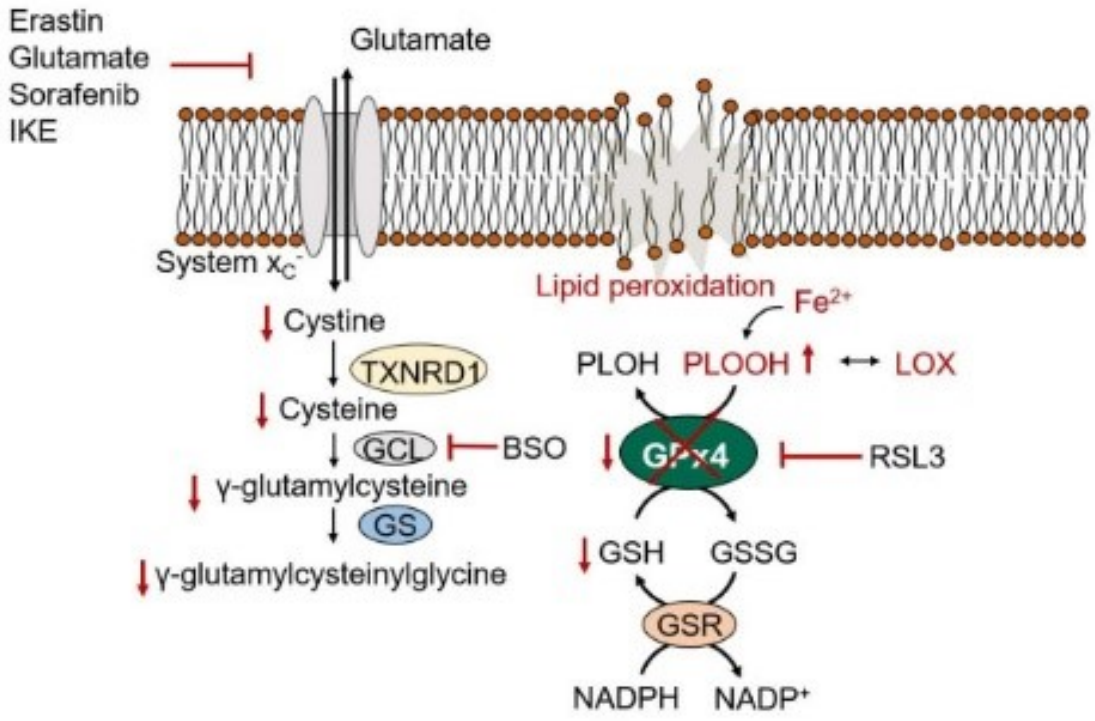

Figure 3. Mechanisms of Ferroptosis induction. See text for details.

Other ferroptosis inducing agents like (1S, 3R)-RSL3 act by directly inhibiting GPx4 activity [5]. RSL3 because of its electrophilic chloroacetamide moiety is competent for a nucleophilic attack to amino acids such as Cys or Selenocysteine (Sec). Yang et al. showed that RSL3 is capable for direct targeting of GPx4, at the level of catalytical Sec , eventually resulting in inhibition of its peroxidase activity [16].

Both the inhibition strategies stress the role of GPx4 as the ultimate controller of ferroptotic cell death.

1.2.2 Positive regulators of Ferroptosis

1.2.2.1.Lipid peroxidation

Cellular membranes lipids are necessarily the principal determinant of ferroptosis, and the degree of unsaturation of lipid bilayers is a crucial determinant of cell sensitivity to ferroptosis, even if the exact mechanism of lipid peroxidation initiation is still unknown. Polyunsaturated

fatty acids are susceptible to oxidative degradation that can lead to loss of integrity of membranes, loss of cellular homeostasis and cell death [17]. As such, lipid peroxidation is seen as the critical event of ferroptosis and susceptibility of hydrogen abstraction from PUFA indispensable for the execution. In this respect it has been elegantly shown that cells pretreated with PUFAs where the heavy hydrogen isotope deuterium substitutes for hydrogen (D-PUFA) were resistant to lipid peroxidation and ferroptosis, due to increased energy of the carbon-deuterium bond over the carbon-hydrogen one [16].

Lipid peroxidation is a complex series of reaction where lipids are degraded to a series of compounds all derived from hydroperoxides. Lipid peroxidation consists of three stages:

i) initiation, when the first radical is produced;

ii) propagation, where oxygen is added in a chain reaction and the number of radicals remains constant;

iii) termination when the number of radicals decreases by radical-radical interaction.

PL-OOH inevitably and continuously produced during aerobic metabolism are also the most important initiators of peroxidative chain reactions, when a lipid radical is formed in the membrane [18]. The initiating free radical is generated from PL-OOH by metals like iron (Fe^{2+}) breaking the O–O bond and forming the extremely reactive alkoxyl radical (PL-O$^{\bullet}$) in a Fenton-like reaction.

$$PL\text{-}OOH + Fe^{2+} \rightarrow PL\text{-}O^{\bullet} + Fe^{3+} + H_2O$$

The alkoxyl radical generates the carbon centered radical L$^{\bullet}$

$$PL\text{-}O^{\bullet} + PL\text{-}H \rightarrow PL\text{-}OH + PL^{\bullet}$$

or, rearranges forming an epoxy group and a carbon centered radical in the fatty acid chain. Irrespective the presence of the epoxy group, the carbon centered radicals in the presence of oxygen forms a lipid hydroperoxyl radical (PL-OO$^{\bullet}$), which further by an H transfer generates another molecule of PL-OOH. When H is donated by a methylenic carbon of divinyl methane moiety of a fatty acid the formed carbon centered radical adds oxygen and propagates lipid peroxidation.

$$PL^{\bullet} + O_2 \leftrightarrow PL\text{-}OO^{\bullet}$$

$$PL\text{-}OO^{\bullet} + PL\text{-}H \rightarrow PL\text{-}OOH + PL^{\bullet}$$

During this propagation phase the number of radicals remains constant. The chain propagation is blocked with H donors, such as tocopherols (TOH) or coenzyme Q substituting for a PUFA. This reaction is defined as chain breaking since the antioxidant radical (e.g. tocopherol) is not reactive enough to efficiently propagate the reaction.

$PL\text{-}OO^{\bullet} + TOH \rightarrow PL\text{-}OOH + TO^{\bullet}$

Since the oxygen addiction to a carbon centered radical is reversible, the chain breaking reaction although limiting propagation, favours the formation of PL-OOH. In this respect the scavenging reaction is also pro-peroxidant since from PL-OOH divalent metal ions initiate a new chain reaction. Thus, it is questionable whether the chain breaking reaction (i.e one electron reduction of $PL\text{-}OO^{\bullet}$) could be relevant for the inhibition of ferrous iron-dependent lipid peroxidation.

The length of the peroxidative chain depends on membrane structure and composition. In general, it is recognised to be very short, propagation being terminated by radical-radical interaction. A typical arrest reaction, resulting in a decreased number of free radicals, is the disproportion of LOO• through the Russell mechanism:

$2\ LOO^{\bullet} \rightarrow LOH + L{=}O + O_2$

This reaction results in a hydroxyl and a keto derivative of fatty acid chain (LOH and L=O), and molecular oxygen is released in an electronically excited state that decays emitting a photon [19].

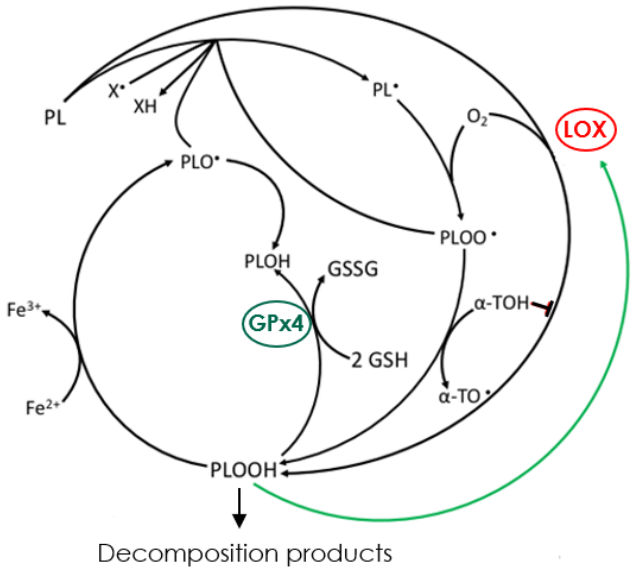

Figure 4. Scheme of lipid peroxidation controlled by GPx4. The phospholipid carbon centered radical (PL•) can be generated by i) an initiating radical (X•) ii) a hydroperoxyl radical (PL-OO•) in propagation reactions iii) a alkoxyl radical (PL-O•) deriving from PL-OOH. Propagation reactions generates PL-OOH, which in turn are reduced by GPx4 into the corresponding alcohol (PL-OH). If not, PL-OOH in a Fenton type of a reaction with Fe^{2+} produces PL-O•. Furthermore, PL-OOH could activate lipoxygenases (LOX) that produces more PL-OOH. PL-OOH generates decomposition products that can react with various nucleophilic residues in protein modifying their functions. Adapted from [20].

PL-OOH are unstable and can generate a complex series of oxidized derivatives and fragmentation products such as reactive aldehyde species [20]. These species may in turn induce lipid, protein and DNA modifications. 4-hydroxynonenal (4-HNE) is the most common and studied molecule, able to modify nucleophilic residues of essential signalling proteins and is detoxified by three aldo-keto reductase family 1, member C (AKR1C1-3). The formation of aldehydes has been suggested to be a critical mechanism for ferroptosis execution since overexpression of AKR1C1 is associated to resistance [21].

Besides slow oxidation linked to oxidative metabolism, PL-OOH can be generated also by lipoxygenases (LOX) that in turn are activated by PL-OOH. LOX catalyzed reaction deeply sensitize cells to ferroptosis by increasing the conversion of lipids into the corresponding hydroperoxides, which anyway requires iron and missing GPx4 activity to occur [22]. This is

in line with studies performed by Seiler et. al.: they proved that 12,15-LOX knock-out cell are less sensitive to cell death [23].

Similarly increased expression of acyl-CoA synthetase long chain family member 4 (ACSL4) and lysophosphatidylcholine acyltransferase 3 (LPCAT3) that increase the amount of PUFA prone to lipid peroxidation sensitize cells to ferroptosis [24,25].

1.2.2.2 Iron

The term Ferroptosis underlines the key role of free-iron for initiation of lipid peroxidation that in turn leads to cell death [4]. It is the cellular pool of redox-active free Fe^{2+}, the so called "labile iron pool" (LIP), having the key role of initiating LPO from LOOH. In details, it participates in Fenton type of reactions operating the cleavage of O-O bond of a phospholipid hydroperoxide (PL-OOH) forming the peroxidation initiating radical.

The relevance of intracellular iron was proved by using chelators, or by adding iron to the growth medium in the form of iron bound to transferrin [26].

Iron is fundamental to life because it participates to redox transitions and interactions with oxygen which is indispensable to cell growth and survival. Iron is indispensable therefore to both life and regulated cell death.

Intracellular iron amount and availability is tightly controlled by iron-regulatory proteins (IRP1 and IRP2), that can sense the cellular concentration of free iron and change the rate of uptake, storage, release and export. Cellular iron uptake occurs via Fe^{3+} loaded transferrin (Tf) that binds to transferrin receptor (TfR) followed by endosomal uptake. In the endosome, the acidification induces the release of Fe^{3+} from Tf, the reduction to Fe^{2+} by STEAP3 protein and the subsequent transfer to the cytosol by divalent metal transporter 1 (DMT1) or ZIP8 and 14 (members of the solute carrier protein family 39) where it gets associated to LIP [27]. LIP Fe^{2+} is either used in biosynthetic pathways or is sequestered by ferritin, an iron storage complex. To maintain iron cellular homeostasis, ferritin can undergo the process of autophagy, thus contributing to ferroptosis as it results in release of free iron [28].

1.2.3 Negative regulators of Ferroptosis

1.2.3.1 PIP, PHGPx, GPx4

GPX4, a selenoprotein originally discovered in 1982 by Ursini et al., catalysing the reduction of PL-OOH [29]. Due to the ability to inhibit lipid peroxidation in liposomes and membranes, the enzyme was first named Peroxidation-Inhibiting-Protein (PIP). PIP's reducing activity on phospholipid hydroperoxides was described operating by a uni-ter ping pong mechanism, similar to the mechanism already defined for GPx1 [30]. However, PIP could also reduce phosphatidylcholine hydroperoxide (PC-OOH), cholesterol and cholesterol ester hydroperoxides inserted in membranes. To underline the enzymatic role of PIP, in 1984 the enzyme was given a name 'Phospholipid Hydroperoxide Glutathione Peroxidase' (PHGPx) [9].

Today eight GPxs are known and PHGPx was systematically classified as glutathione peroxidase 4 i.e. GPx4 [31].

1.2.3.1.1 GPx4 structure

GPx4 is a monomeric protein that at the tertiary protein structure level bears an extended thioredoxin fold [32]. This α/β motif is also common to thioredoxins, glutaredoxins, glutathione S-transferases and Dsba, which do not share any specific function. However, all of them belong to the enzymatic class of oxidoreductases.

The thioredoxin fold consists of four stranded beta-sheets and three flanking alpha-helices yielding a two layers α/β/α sandwich with a β1α1β2α2β3β4α3 secondary structure pattern. In GPx family members, the thioredoxin fold contains additional elements: two β-sheets at the N-terminus and one additional α-helix and β-sheet between β2 and α2. Furthermore, in tetrameric GPxs there is an extra aminoacid stretch positioned between α2 and β3, deleted in monomeric GPx4.

The active site of all the GPx lies in a flat area of the protein surface making it accessible to complex lipid hydroperoxides. The redox active Se is at hydrogen-bonding distances from three strongly conserved residues, important for the catalysis: a Gln, Trp and Asn, located in distant loops in the primary structure. In addition, analysis of human GPx4 structure shows that besides the positively charged area close to the peroxidatic Sec, there is another cationic area that is expected to contribute to the binding of exposed polar heads of phospholipids.

1.2.3.1.2 GPx4 kinetics and catalytic mechanism

Glutathione peroxidases are enzymes relying on either Sec or Cys catalysis [33]. In mammals, the first four (GPx1-4) and the sixth (GPx6) homologs contain Sec in catalytically active site, while in the other three enzymes (GPx5, GPx7 and GPx8) Cys substitutes for Sec.

GPx4 enzymatic catalysis follows the kinetic pattern of the first described SecGPx - GPx1, regardless the different substrate specificity. The catalytic mechanism is described as a ping-pong mechanism consisting of two events: oxidation of the reduced enzyme by a hydroperoxide, followed by a two-step reduction of the oxidized form by GSH [34]. As described in Figure 3, the Sec selenol (E) in the active site is oxidized by R-OOH substrate, being reduced into the corresponding alcohol, followed by the reduction of the oxidized enzyme. The oxidized intermediate (F) is reduced in two subsequent steps: the first yielding the glutathionylated enzyme, i.e a selenodisulfide; in the second, selenodisulfide is reduced by a second GSH molecule forming GSSG and releasing the reduced catalytic selenium in the form of selenol (E) ready for the next cycle.

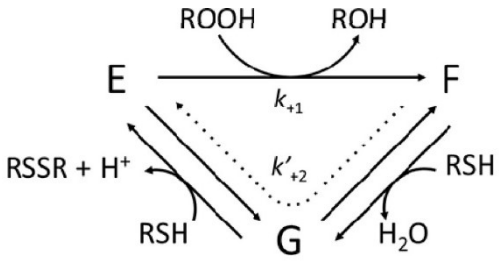

Figure 5. Scheme of GPx4 catalysis. See text for details.

The catalysis of GPx does not fulfils the Michaelis-Menten reaction kinetics. The reactive catalytic moiety suggests that the redox transitions occurring in the catalytic pocket are faster than the formation of typical enzyme-substrate complex. Thus, SecGPx kinetics theoretically reaches infinite Vmax and Km values. The Dalziel equation that describes this kinetic pattern is:

$$[E0] / v0 = 1 / k'^{+1} \cdot [ROOH] + 1 / k'^{+2} \cdot [GSH]$$

where k'^{+1} and k'^{+2} are the apparent rate constants for the net forward oxidative and reductive part of the catalytic cycle, respectively. For the SecGPxs homologues the apparent rate constant

for the oxidizing step (k_{+1}) is among the fastest ever determined for bimolecular enzymatic reactions (around 10^8 M^{-1} s^{-1}). The reductive part is the rate-limiting step of the catalytic cycle.

Recently, the catalytic cycle of GPx4 was described in atomic detail by density functional theory (DFT) procedure which allowed to obtain the energetic profile for the entire catalytic cycle, including intermediates and transition states [35]. The results showed that during the oxidative step of the catalytic cycle, a deprotonated intermediate of selenol is formed which is gradually oxidized to selenenic acid. Lack of activation energy in this step complies with the elevated k_{+1} value measured by steady-state kinetics for the oxidizing step and establish that the selenenic acid derivative of Sec is indeed the oxidized Se form in GPx. The energetic profile of CysGPx is similar to the one described for SecGPx, except for the formation of sulfenic acid instead of selenenic acid and comprehensive higher activation energies, which is in agreement with the lower efficiency of sulfur versus selenium catalysis.

During the reductive step of the catalysis, the DFT calculations confirmed that the enzyme forms the selenenylsulfide (or disulfide for CysGPx) intermediate which in the presence of a second molecule of thiol regenerates the ground state enzyme. The second reductive step having the highest activation energy is the rate-limiting reaction of the cycle. In addition, DFT calculations implied that the lack of reducing substrate leads to an oxidized intermediate 2 atomic mass units lighter that the reduced ground form. This intermediate contains selenium integrated as selenenylamide (Se-N) in a relaxed 5 or 8-membered ring generated by the interaction of selenenic acid with the downstream peptide nitrogen at the backbone of the enzyme. When the reducing substrate becomes available again, the thiolysis of the Se-N bond leads to the formation of Se-disulfide, which continues the catalytic cycle. Thus, the formation of selenylamide protects SeGPx from inactivation by over-oxidation. Notably, an analogous formation of sulfenylamide has been ruled out by quanto-mechanical calculation and it has been not analitycally detected. This further underlines the notion that the important advantage of selenolate- versus thiolate-based catalysis lies in its resistance to overoxidation.

Ingold et al. using a transgenic animal model confirmed the advantage of selenolate-based GPx4 catalysis in respect to thiolate-based catalysis [36]. In this work it has been demonstrated that Cys-GPx4 variant is subjected to over-oxidation and inactivation, whereas Sec-GPx4 is resistant to oxidative inactivation thus being indispensable for controlling ferroptotic cell death. In fact, substitution of Cys for Sec leads to severe lethal alterations in embryogenesis and, only in a specific genetic background, a deadly neonatal neurodegeneration in this animal model.

At cellular level, the contemporary deletion of all 25 selenoproteins don't impact on cell survival until a minimal residual GPx4 activity is conserved in cells expressing the Cys-GPx4 variant.

1.2.3.2 GSH

GSH, the reducing substrate of GPx4, is a molecule indispensable for life. Consistently, mice lacking γ-glutamylcysteine ligase (GCL), the rate-limiting enzyme of GSH synthesis die at the same developmental stage as GPx4 knock-out mice [37]. Due to its relevance, GSH content inside the cell is tightly controlled at multiple levels, i.e. uptake of single aminoacids, synthesis and recycling.

Furthermore, GSH preserves cell from ferroptosis as demonstrated by studies on cancer cells using the small molecule erastin, which irreversibly blocks the cellular import of cystine through system Xc-, necessary to sustain GSH levels [4]. Since Xc- is a bidirectional antiporter, the net flow of metabolites is controlled by the concentration of Glu and Cys. So, high concentrations of extra cellular glutamate inhibit cystine import and cause cell death by GSH deprivation. This modality of toxicity and cell death is particularly important for neurons and was first described about 20 years ago and named oxytosis. Oxytosis is characterized by GSH depletion, LOX activation and increased lipid peroxidation, common features of Ferroptosis. Oxytosis and Ferroptosis probably represent the same form of RCD [1].

In addition to system Xc-, cells use other amino acid transporters for cysteine uptake or, alternatively, generate Cys from methionine by the transsulfuration pathway. Transsulfuration pathway converts methionine to homocysteine which further gets converted to cystathionine and finally Cys. This pathway, activated by cystenyl-tRNA synthetase (CARS) knock down, has recently been shown to have a role in the protection against ferroptosis induced by system Xc- inhibitors [38]. Furthermore, cystathionine has recently emerged as a novel substrate of the system Xc- able to regulate extracellular glutamate concentration and cystine availability in the brain. Thus, exchange of cystathionine through system Xc- increases intracellular GSH concentration thereby contributing to the maintenance of the oxidative homeostasis of the cell.

Moreover, GSH biosynthesis is under the control of Nuclear factor erythroid 2-related factor 2 (Nrf2) transcription factor, the key regulator of the cellular response against different issues, including oxidative stress [39]. Electrophiles created during oxidative stress will react with nucleophilic Cys residues of Kelch like-ECH-associated protein 1 (Keap1) and disrupt the constant ubiquitination of Nrf2. The accumulated Nrf2 will transfer to the nucleus and

upregulate the expression of GCL and GSH synthesis. Similarly, Nrf2 upregulates the expression of system Xc- and create an efficient reducing cystine/cysteine cycle thereby protecting from cell death.

To prevent cell death, some cells like astrocytes, can secrete GSH into extracellular space by multi-drug resistance proteins (MRP) and provide GSH for other cells like neurons. In that case, secreted GSH is cleaved by γ-glutamyltranspeptidase (GGT) releasing Glu and cystenylglycine. GGT transfers Glu to other amino acids and the cystenylglycine dipeptide is hydrolysed by a dipeptidase (DP) releasing Cys and Gly. Free Cys and Gly, as well as γ - glutamyl amino acids, can then be taken up by various transporters from neurons and used for GSH synthesis.

Besides GSH, MRPs can export oxidized glutathione (GSSG), as well as GSH adducts generated by glutathione transferases (GST). In that manner GSTs detoxify a variety of aldehydes and electrophiles created during cell metabolism. In fact, the induction of MRP1 has been demonstrated to be neuroprotective. Nevertheless, in some studies the major reported biological effect of MRP is the depletion of intracellular GSH and this intrinsically represents a risk of poorly controlled oxidations and related toxicity and death [40].

1.2.3.3 FSP1, a GSH-independent inhibitor of ferroptosis

Besides the "classical" anti ferroptotic pathway represented by GPx4-GSH axis, in 2019, two groups identified a protein named FSP1 (ferroptosis suppressor protein 1), previously known as AIFM2 (apoptosis-inducing factor mitochondrial 2) as a ferroptosis suppressor that operates independently of GPX4 at the level of the plasma membrane [41,42]. FSP1 is recruited to the plasma membrane by myristoylation, where it functions as a NADPH-dependent CoQ oxidoreductase that reduces CoQ10 (also known as ubiquinone-10). Reduced CoQ10, in turn, acts as a lipophilic radical-trapping antioxidant that blocks the propagation of lipid peroxides and prevent ferroptosis. Thus, the NADPH-FSP1-CoQ10 pathway is a strong inhibitor of lipid peroxidation and ferroptosis and is complementary to GPx4-GSH system (Figure 6).

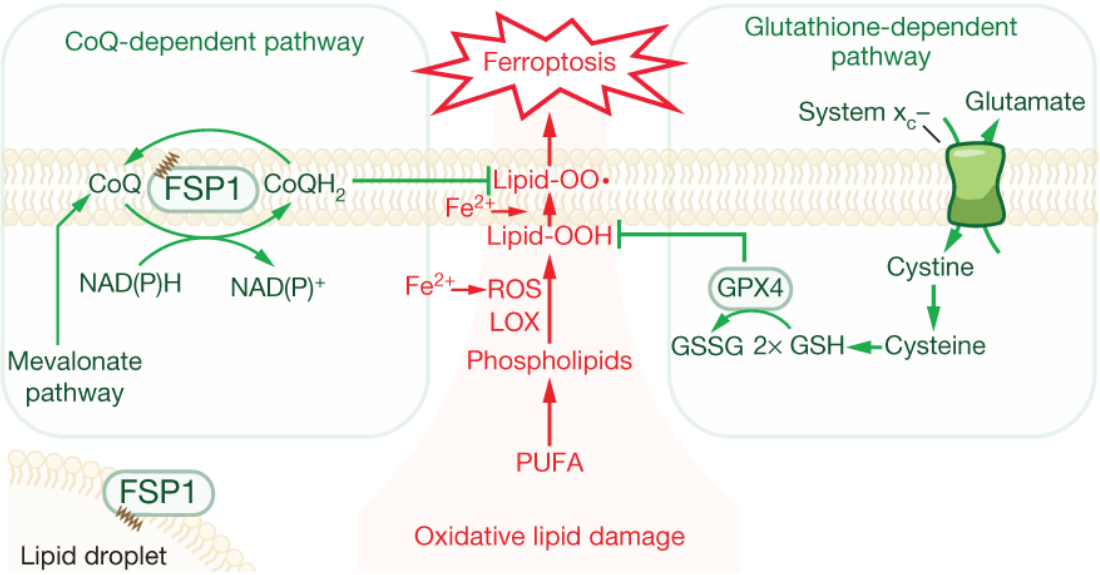

Figure 6. Model illustrating the mechanism by which FSP1 and GPx4 suppress ferroptosis. Adapted from [42].

1.2.4 Contribution of metabolism to Ferroptosis

The contribution of cysteine, iron, lipid species and activated oxygen species to ferroptosis suggests a strong relationship between ferroptosis and metabolism. An intimate and intricate connection between metabolic pathways and ferroptosis has been revealed by recent studies [30,26, 43]. For instance, it is still a matter of discussion whether and how autophagy, that is a catabolic process aimed to maintain the cell homeostasis in response to different issues, can promote cell death. According to recent findings, amino acid starvation, known to trigger autophagy, promotes a rapid ferroptotic form of cell death, as outlined by the needing of transferrin and glutamine in the experimental conditions, where the specific deprivation of cysteine triggers cell death. The requirement of iron and the protective role of cysteine clearly point out ferroptosis as the mechanism of cell death in these conditions, and the specific form of autophagy involved is the ferritinophagy, based on degradation of ferritin with release of iron in the labile iron pool.

In addition, the need of glutamine metabolism, or glutaminolysis, for cystine deprivation-induced ferroptosis links ferroptosis to oxidative metabolism. Glutamine is a crucial anaplerotic metabolite that feeds the mitochondrial tricarboxylic acid (TCA) cycle, thus increasing the rate of mitochondrial respiration and the potential for the generation of oxygen activated species. Thus, a normal metabolic function of mitochondria appears to be implicated in ferroptosis. Also glucose, the main fuel of TCA cycle can modulate ferroptosis, since

recently it has been demonstrated that glucose starvation inhibits ferroptosis. But, this seems to be mainly due to the activation of the energy sensor AMP activated kinase (AMPK), while it is not clear the involvement of TCA cycle and mitochondrial respiration. In addition, it is not clear if mitochondrial metabolism promote ferroptosis by generating specific lipid precursors for PLOOH synthesis (intermediates of the TCA cycle participate in lipogenesis) or via the generation of activated oxygen species as by-products of oxidative metabolic reactions [7].

1.2.5 Relevance of ferroptosis in physiological and pathological conditions

Like other form of regulated cell death, ferroptosis has been presumed to be involved in physiological and pathological events since its characterization. To date, the physiological relevance of ferroptosis is hypothesized but remains unclear, with little evidences in tumor suppression and immune surveillance [7].

The importance of ferroptosis in disease, on the contrary, is well documented and ferroptosis dysregulation is classically linked to cancer, neurodegeneration, and ischemia-reperfusion injury [44]. Growing studies highlight the involvement of ferroptosis also in liver and lung fibrosis, bacterial infections like sepsis and tuberculosis, as well as viral infections [7].

Irrespective of the different pathological condition, the regulated character of ferroptosis represents an appealing approach for therapeutic strategy. For instance, in the case of cancer, ferroptosis induction-based therapies are under investigation. In this scenario, several untargeted nanoparticle-based strategies to deliver iron, peroxides and other toxic cargoes to kill tumour cells have been tested.

AIM

Ferroptosis is a form of regulated cell death operated by iron-dependent lipid peroxidation. Ferroptosis is primed by the missing or insufficient activity of the Glutathione Seleno-Peroxidase 4 (GPx4), which catalyzes the glutathione (GSH)-dependent reduction of lipid hydroperoxides to the corresponding alcohols. Besides GPx4 inactivation, Ferroptosis occurs when other conditions are satisfied: -oxygen metabolism leading to the continuous formation of traces of LOOH from phospholipid-containing polyunsaturated fatty acids; - availability of ferrous iron from the labile iron pool. Consistently with the critical role of the traces of LOOH, we recently proposed that Ferroptosis follows the loss of homeostatic control between the oxidative challenge posed by aerobic metabolism and GPx4 activity [42]. The working hypothesis, supported by acknowledged chemical mechanisms, was that O2•- arising from aerobic metabolism accounts for the formation of the tiny amounts of LOOH sparking iron-dependent LPO and thus Ferroptosis.

A functional link between Ferroptosis and metabolism was proposed to rely on glutamine metabolism, Krebs cycle, and mitochondrial respiration [26,43], but the molecular mechanisms remain almost completely unknown.

This work aimed to shed light on the relationship between aerobic mitochondrial metabolism and ferroptosis induced by GSH depletion, focusing on the site of production and the mechanism of reactions leading to the indispensable formation of traces amounts PL-OOH from which iron initiates LPO when GPx4 activity is insufficient.

MATERIAL AND METHODS

3.1. Cell culture and reagents

HT1080 cells (ATCC® CCL 121™) were cultured in Dulbecco's Modified Eagle's Medium (DMEM), containing glucose 1 g/l, 4 mM Glutamine, 1 mM Sodium Pyruvate and supplemented with 10% (v/v) fetal bovine serum, 1% (v/v) Penicillin/Streptomycin (Gibco). Erastin and ferrostatin-1 (Fer-1) were purchased from Selleckem and the other chemicals from Sigma-Aldrich, if not otherwise specified. In the experiments where the energetic substrates were omitted, DMEM without glucose, glutamine and pyruvate, supplemented with 10% (v/v) FBS, 1% (v/v) penicillin/streptomycin (Gibco) was used (eDMEM). The fluorescent probes Bodipy 581/591C11, Mitosox and Calcein AM, were purchased from Invitrogen. Anti-GADPH, anti-βactin antibodies were from Sigma-Aldrich; anti-pyruvate dehydrogenase complex-E1α phosphoS293 was from Merck; anti-pyruvate dehydrogenase complex-E1α, anti-lipoamide dehydrogenase antibody from Abcam; HRP conjugated anti-mouse (sc-516102) and anti-rabbit (sc-2004) antibodies from Santa Cruz Biotechnology.

3.2. Cell viability assay

Cells were seeded onto a 96-well plate at a density of 5,000 cells/well or 50,000 cells/well, for the sub-confluent (less than 50% confluency after 24 h) or confluent condition, respectively. 24 hours later, the cells were treated in the medium used for experiment containing erastin, RSL3 or CDDO at the indicated concentrations. After 24 h, cell viability was assessed by the resazurin assay (Sigma-Aldrich), as indicated by the manufacturer. Fluorescence was evaluated using a plate reader (FluoScan-ThermoSystem, ex. 544, em. 590 nm) where the resazurin reduction rate was assessed as A.F.U/min and expressed as % vs control.

3.3. Measurement of total GSH

Cells were seeded onto a 6-well plate (150,000 cells/well) and cultured for 24 h. After treatment, cells were washed with PBS and lysed in buffer containing 0.1 M KH2PO4/K2HPO4, 0.15 M KCl, 0.05%, CHAPS pH 7 and protease inhibitors. Total amount of GSH was measured according to the enzymatic method first described by Tietze [45]. The reaction started by adding 10 µL of the sample in buffer containing 0.1 M NaH2PO4/Na2HPO4 pH 7.4, 1 mM EDTA, 0.14 mM DTNB, 0.1 mM NADPH and 0.8 units/mL of glutathione reductase.

3.4. Measurement of the oxygen consumption rate

The oxygen consumption rate (OCR) was determined using a Seahorse Bioscience Extracellular Flux Analyzer (XF24-3 Agilent). Cells were plated on dedicated 24 well plates (35.000 cells/well) and allowed to attach overnight. The following day cells were washed 2 times in Seahorse XF DMEM Medium, pH 7.4 assay media (Agilent Technologies) before treatment. Oxygen consumption rates were compared between basal measurements and following addition of FCCP or antimycin. OCR was normalized for the number of living cells based on Calcein AM incorporation. Fluorescence was recorded after 30 min by FluoScan plate reader using 490 nm excitation filter and 520 nm emission. For measurement of OCR in cells in plates at different density, the fluorescence plate reader approach MitoXpress Xtra oxygen consumption assay, was used. Rates of oxygen consumption were calculated from the changes in fluorescence signal over time. To this end, HT1080 cells were seeded at low (10.000/well) and high (50.000/well) density in a 96 wells plate (Eppendorf), avoiding outside wells and filling the moat with 5 mL PBS. The day after, the assay was performed following the manufacturer's protocol. Fluorescence decay was measured kinetically in a microplate reader (EnVision - PerkinElmer) at 37 ◦C in time-resolved fluorescence (TR-F) mode using a filter set as follows, 380 nm excitation and 620 nm emission filters, window time 100 μs, delay 40 μs.

3.5. Measurement of C11 bodipy oxidation

Cells were seeded onto a 12-well plate (80,000 cells/well) and the next day suspended with eDMEM containing the indicated concentration of pyruvate. After 7 h, cells were incubated for further 60 min with 581/591C11 Bodipy (1 μM) before harvesting by trypsinization. Subsequently, cells were resuspended in 300 μL PBS for flow cytometry analysis (BD, FACSCantoII™, equipped with a 488 nm excitation laser). Fluorescence of oxidized C11-BODIPY was recorded at 535 nm. At least 10,000 cells were acquired per sample using BD FACSDiva™ Software. To correct for autofluorescence, the median fluorescence intensity (MFI) of an unstained sample was subtracted.

3.6. mRNA silencing

For silencing of PDC E1 or PDC E3 subunits -also named Pyruvate Dehydrogenase (PDH) or Dihydrolipoyl Dehydrogenase (DLD)- HT1080 cells were plated at 50% of confluency and subjected to transfection with LipofectamineTM RNAiMAX (Invitrogen) 24 h later, according

to the manufacturer's instructions. For PDC E1 silencing one MISSION® Predesigned short-interfering RNA (siRNA) (SASI_Hs01_00082458, Merck KGaA, or MISSION® universal negative control (SIC001) were used, while for the PDC E3 subunits, one predesigned Dicer-Substrate siRNA (hs.Ri. DLD.13.2, Integrated DNA Technologies) or negative control (DS NC1) were used. The final concentration of RNA duplex was 30 nM. For cell viability assays, 24 h after transfection cells were plated onto a 96-well plate (5000 cells/well) and the next day suspended in the medium used for experiment containing erastin at the indicated concentration. Silencing was verified by Western Blot and by qRT-PCR.

3.7 qRT-PCR mRNA quantification

Total RNA of control or silenced cells were extracted using the Total RNA Purification Kit (Norgen Biotek Corp.) and retrotranscribed using the SuperScript® III Reverse Transcriptase (Thermo Fisher). Obtained cDNA was analyzed in triplicate to evaluate the gene expression in qRT-PCR using SensiFAST SYBR No-ROX Kit (Bioline Reagents Ltd). The real-time PCR analysis was performed by the Rotor-Gene 3000 (Corbett Research) and the results were normalized against the housekeeping gene hypoxanthine-guanine phosphoribosyl transferase (HPRT).

Gene name	**Primer Forward sequence (5'→3')**	**Primer Reverse sequence (5'→3')**
PDHE1	CAACATGGCAGCTTTGTGGA	CTCTCGGACGCACAGGATAT
DLD	GTTGAAGGAATGGCTGGTGG	TGCCCAAGGATCTTCACCAT
HPRT	CCTGGCGTCGTGATTAGTGAT	AGACGTTCAGTCCTGTCCATAA

3.8. Western blotting

Proteins of cell lysates were measured by the Bradford method and 20 μg of samples were subjected to SDS-PAGE on precast NuPAGE™ 4-12% Bis-Tris Protein Gels (Invitrogen) and further transferred to a nitrocellulose membrane for Western blot analysis. After blocking with 3% bovine serum albumin at room temperature, membranes were incubated with the appropriate antibodies overnight. Immunodetection was carried out with the ECL Western Blotting Substrate on the ImageQuant LAS 4000 imaging system (GE Healthcare). Membranes, when required, were reprobed with other primary antibodies.

3.9. Mitochondrial $O^{2\bullet-}$ determination

HT1080 cells, seeded the day before (80,000 cells/well in 12-wells/ plate) were incubated for 8 h in eDMEM or eDMEM containing 10 mM pyruvate and treated with erastin. Thirty minutes before detachment, 1.25 μM MitoSOX was added. Right after trypsinization and washing, flow cytometry analysis was performed (BD, Fortessa-X20 ecc 488, em 610 nm). Autofluorescence correction and analysis were performed as described in paragraph 2.5.

3.10. Statistical analysis

All graphs and statistical analyses were performed using Graph Pad Prism 9. (*GraphPad* Software, Inc., San Diego, CA). In viability experiments, the normalized data -at least 8 replicates for each concentration-were analyzed by comparing the results of two equations: a) [Inhibitor] vs. normalized response -constant slope and b) [Inhibitor] vs. normalized response - variable slope [24]. The best-fit parameters were utilized to express the E50, i.e. the dose of erastin eliciting death in 50% of the cells. Differences between groups were considered statistically significant when *P* value was less than 0.05 (*$P < 0.05$; ***$P < 0.001$;****$P < 0.0001$).

RESULTS

4.1 Cell density regulates sensitivity to ferroptosis

Mitochondrial activity emerges as a key indispensable determinant of ferroptosis [43,44,46]. In fact, oxygen activation and metabolism fulfil the biochemical features to be a reasonable source of tiny amounts of LOOH required for initiating iron-dependent lipid peroxidation on unsaturated membranes.

To explore the connection between ferroptosis and aerobic metabolism we used as a suitable model ferroptotic cell death, primed by erastin in HT1080 cells. Erastin, by inhibiting cystine import system Xc, decreases the cellular level of GSH and, consequently, GPx4 activity. We evaluated the efficiency of a given metabolic condition from the sensitivity to ferroptosis induced by erastin. To this end, we adopted as semi-quantitative index, the concentration of erastin that reduced viability to 50% (E_{50}).

In the first set of experimental work, we achieved evidence for a role in ferroptosis of the mitochondrial α-ketoacid dehydrogenase complexes (αKDC). The highly regulated pyruvate dehydrogenase complex (PDC) has been specifically addressed as a prototype of this family of similar enzymes.

First, we confirmed previous findings that non-confluent, fast proliferating cells are more sensitive to ferroptosis than cells grown at the confluence (Figure. 7A) and likely connected to the faster oxygen consumption rate (Figure. 7B). Furthermore, we observed that ferroptosis does not take place when a “empty” DMEM, devoid of the major energetic substrates, i.e. glucose, glutamine and pyruvate (eDMEM), substitutes for DMEM (Figure. 7C). Of course, missing energetic substrates causes cell death by energetic starvation, although in a time much longer than that in our experiments. We finally ruled out the option that metabolism could alter the kinetics of GSH depletion showing that in the two extreme metabolic conditions adopted GSH is depleted at the same rate (Figure. 7D). The ferroptotic nature of the observed cell death was validated by Ferrostatin (Fer-1), the most specific ferroptosis inhibitor.

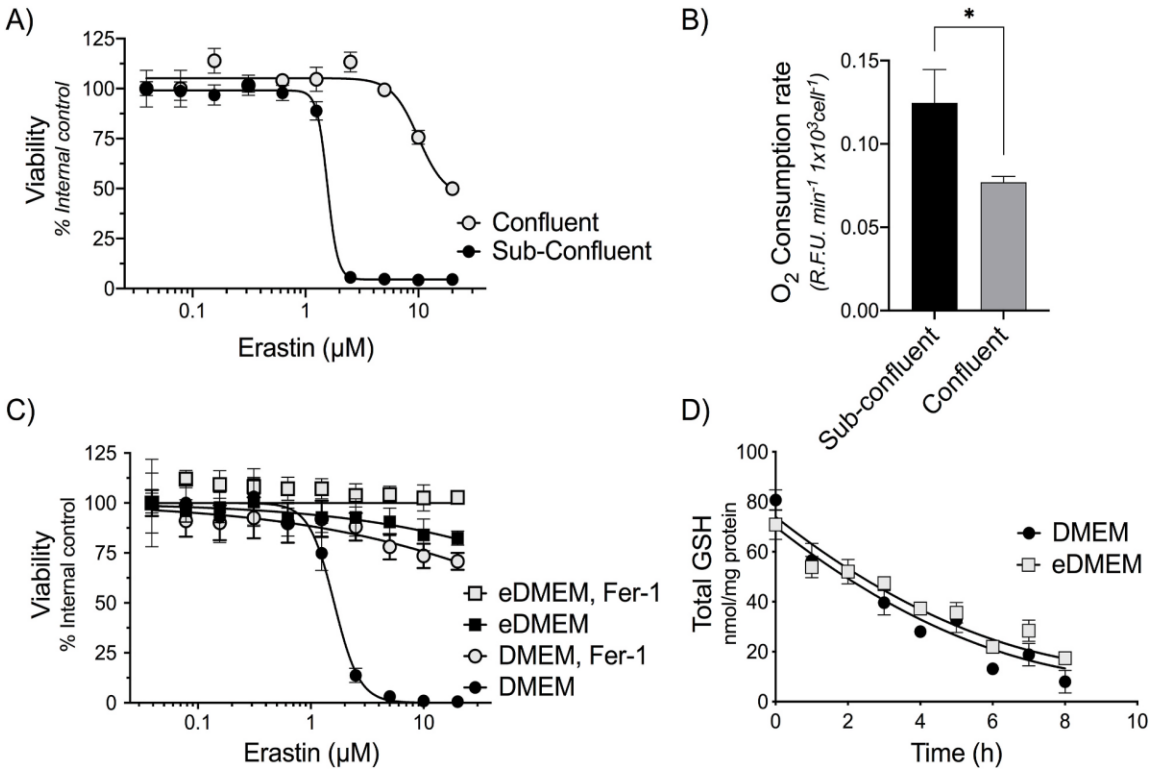

Figure. 7. Cell density and energetic substrates impact on sensitivity to Ferroptosis. Cells were plated at a confluent (50,000 cells/well) or a sub-confluent (5000 cells/ well) density, and the day after DMEM containing erastin substituted for DMEM. Incubation further continued 24 h. Cell seeded at a confluent density are more resistant to Ferroptosis (A), and have a lower oxygen consumption rate (B). In the absence of the energetic substrates -glucose, glutamine, pyruvate- (eDMEM) the resistance to ferroptosis is deeply increased (C). The kinetics of GSH depletion by erastin is the same in DMEM or eDMEM (D). Viability was measured as resazurin reduction rate and expressed as % of untreated cells (control), OCR was measured by MitoXpress Xtra oxygen consumption assay. Mean ± SD of three independent experiments of eighteen replicates for each condition. Significance calculated by unpaired T test, $*P < 0.05$.

4.2. The mitochondrial respiratory chain is not involved in Ferroptosis

Once established that in our experimental model oxidative metabolism is an indispensable constraint of ferroptosis, we first explored whether electron flow through the respiratory chain might have a role in producing the oxidative challenge priming ferroptosis by decreased GSH. By blocking electron transport chain either with antimycin, which targets complex III, or with FCCP, a potent uncoupler of mitochondrial oxidative phosphorylation, used at a concentration sufficient to obtain a decreased or increased oxygen consumption rate (Figure. 8A), we didn't modify the E_{50} value of erastin (Figure. 8B and 8C). This indicated that, at least in our

experimental conditions, the rate of electron flow in the respiratory chain does not significantly impact on sensitivity to Ferroptosis.

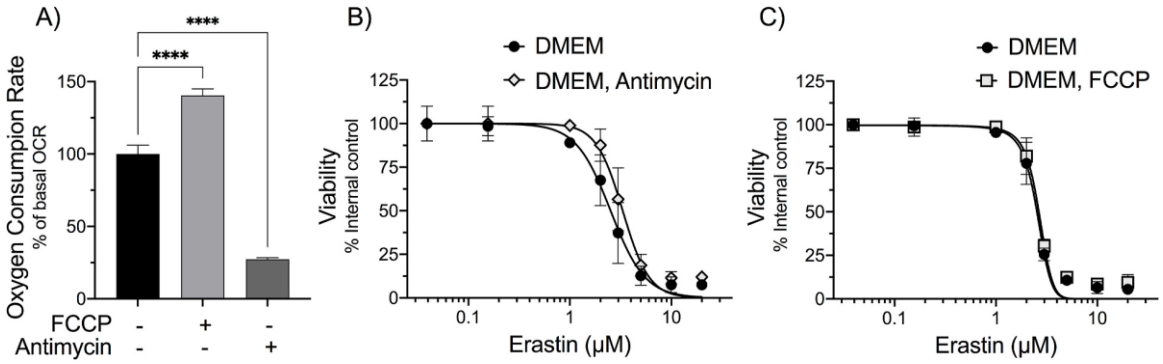

Figure. 8. Electron flow in mitochondrial respiratory chain does not affect sensitivity to Ferroptosis. Neither 0.5 μM antimycin that decreases the OCR, nor 0.3 μM FCCP that increases it (A), modify the sensitivity to ferroptosis induced by erastin (B–C). The OCR was measured using Seahorse Bioscience Extracellular Flux Analyzer. Cell viability was assessed in sub-confluent cells by resazurin. Mean ± SD of three independent experiments. Significance calculated by ANOVA with Sidak's multiple comparison test, $****P < 0.0001$.

4.3 Role of the energetic substrates in erastin-induced ferroptosis

Then, we moved to investigate the role of TCA cycle, and, in this respect, we analysed the effect of each substrate by adding it to eDMEM in the concentration of DMEM. We confirmed the critical role of glutamine, seemingly via glutaminolysis, and of other intermediates of TCA cycle (Figure 9). These data are in agreement with the role of the activity of mitochondrial α-keto acid dehydrogenases as critical players of cell sensitivity to ferroptosis.

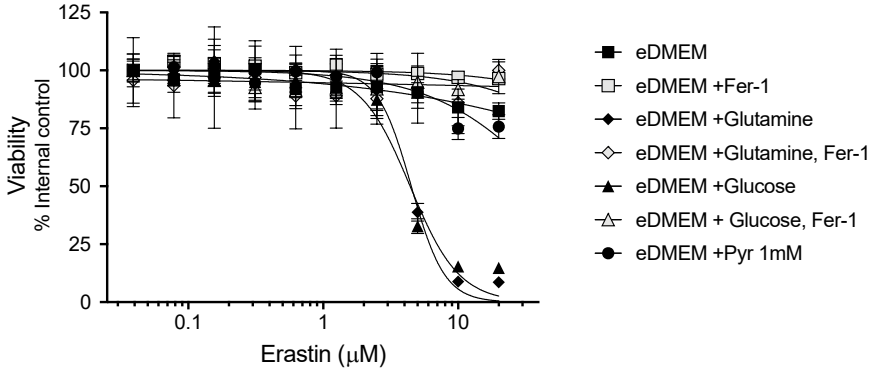

Figure. 9. Energetic DMEM substrates promote Ferroptosis. Cells were plated at a sub-confluent density and 24 hours later eDMEM containing the indicated substrate and erastin substituted for DMEM and further incubated for 24 h. Concentrations were as follows: 5.6 mM glucose, 4 mM glutamine, 1 mM pyruvate. Specificity for

ferroptosis was tested by 5 μM Fer-1. Cell viability was assessed by resazurin. Mean ± SD of three independent experiments of eight replicates for each erastin concentration.

4.4 Role of Pyruvate Dehydrogenase Complex (PDC)

We resorted, therefore, to focus on pyruvate, the main intermediate of the aerobic metabolism of glucose. We observed that in HT1080 cells, pyruvate, at higher concentration, supports erastin-induced ferroptosis: by increasing pyruvate concentrations, we observed a clear inverse relationship with the E_{50} of erastin (Figure. 10A). In agreement with the observed pro-ferroptotic effect of pyruvate, the oxidation of BODIPY C11 also increased, probing the formation of the lipid hydroperoxyl radicals, intermediates of lipid peroxidation (Figure 10B). Next, we addressed whether pyruvate could support the initial formation of $O_2^{\bullet-}$, the likely precursor of the traces of LOOH indispensable to the initiation of iron-dependent lipid peroxidation.

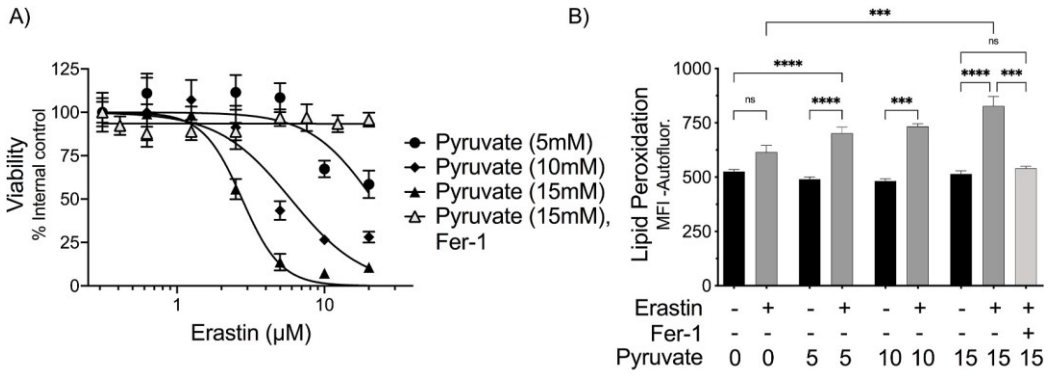

Pyruvate (mM)	5	10	15
E_{50} (μM) ± *S.E.*	21.4±2.7	5.9±0.7	2.7±15

Figure. 10. Pyruvate supports lipid peroxidation and Ferroptosis induced by erastin. Increasing pyruvate concentration in eDMEM increases sensitivity to ferroptosis, evaluated as erastin E50 (A), and oxidation of the lipid peroxidation probe C11 Bodipy (B). Bodipy oxidation was followed by flow-cytometry analysis after 8 h incubation in the presence of 5 μM erastin. When present, Fer-1 was 5 μM. Mean ± SD of three independent experiments of five replicates for each condition. Significance calculated by ANOVA with Sidak's multiple comparison test, ****P < 0.001;*****P < 0.0001.*

Since available evidence indicates αKDC as a relevant source of $O_2^{\bullet-}$ in isolated mitochondria [49,50], we specifically addressed the role of the pyruvate dehydrogenase complex (PDC) in intact cells.

Pyruvate dehydrogenase complex (PDC) encompasses multiple copies of three components: pyruvate dehydrogenase (E1), dihydrolipoyl acetyltransferase (E2) and dihydrolipoamide dehydrogenase (E3). The PDC share the same global structure and uses the same coenzymes as α-KG dehydrogenase complex (OGDC) and branched-chain keto-acid dehydrogenase complex (BCKDC). α-keto acid dehydrogenase complexes have different keto-acid specificity and catalyze the same sequence of reactions, via corresponding acyl-CoAs and NADH (Figure 5). The first reaction, the decarboxylation of the keto-acid, is performed by a specific keto-acid E1 subunit using the cofactor thiamine pyrophosphate (TPP). Then the E2 dihydrolipoamide acyltransferase transfers the formed acyl group to CoA. The third reaction, catalysed by E3 dihydrolipoamide dehydrogenase, operates the oxidation of dihydrolipoamide bound to E2 and requires FAD and NAD^+ as final electron acceptor. Subunit E3 is identical in each complex, while E1 and E2 are different proteins using the same cofactors.

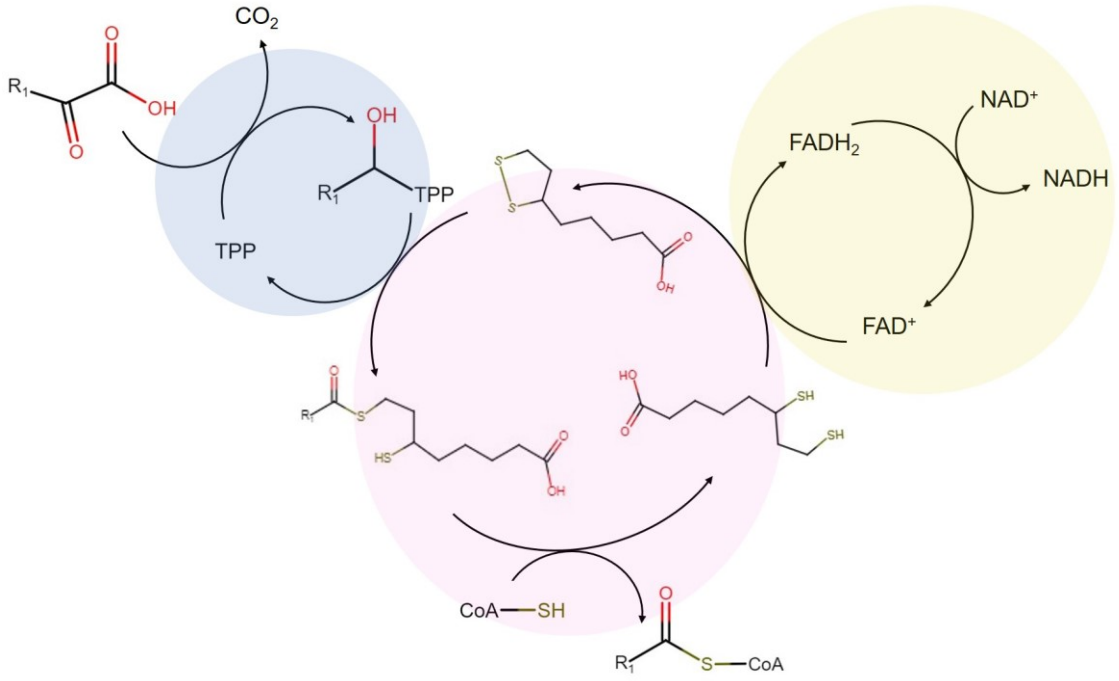

Figure 11. Reaction mechanism of α-keto dehydrogenases

α-Ketoacid dehydrogenase complexes consist of three subunits: keto acid dehydrogenase E1 (blue circle), ketoacid transacylase E2 (pink circle) and dihydrolipoamide dehydrogenase E3 (yellow circle). These complexes catalyse the reactions of decarboxylating the α-keto acid substrate to produce CO_2, acyl CoA and NADH. The reaction performed by E1 is the thiamine pyrophosphate (TPP) dependent decarboxylation of the α-ketoacid yielding an TPP-intermediate. This reaction is followed by the transfer of reactive intermediate to a lipoyl moiety (LA-S2) on the E2 subunit creating an acylated dithiol group. The E2 then transfers the acyl intermediate to CoA forming an acyl-CoA and dihydrolipoamide (LA-(SH)2). FAD on the E3 subunit readily oxidizes the lipoyl group on the E2 subunit and generates NADH through coupled reactions of $FADH_2$ and NAD^+.

We transiently silenced either the E1 subunit, which forms the hemithioacetal that undergoes decarboxylation, or the E3 subunit, the dihydrolipoyl dehydrogenase (DLD) that oxidizes back reduced lipoate to complete the catalytic cycle.

Consistently with the hypothesis, downregulation of the E1 subunit of the PDC, which is specific to this complex, markedly increased the E_{50} value in the presence either glucose or its metabolite pyruvate (Figure. 12A and 12B), while a less pronounced increase of the E_{50} value was observed in DMEM (Figure. 12C). Also this is consistent with observation that the aerobic metabolism of glutamine in DMEM contributes to erastin-induced ferroptosis [3,4].

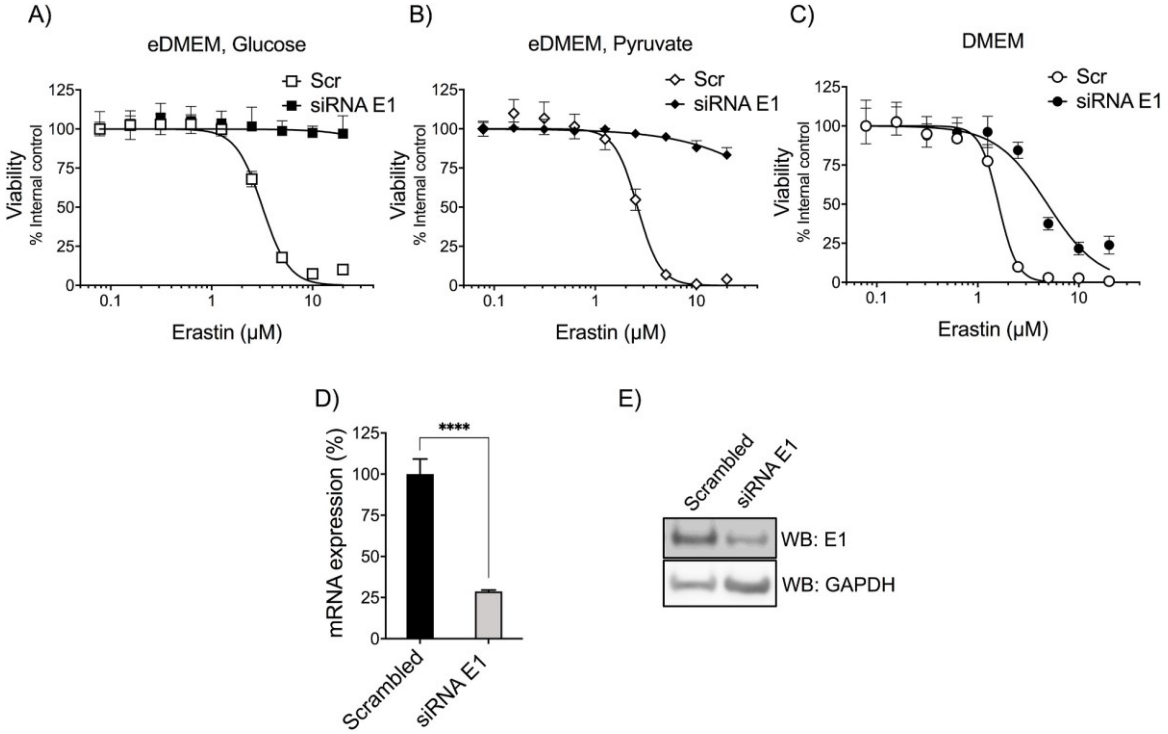

Figure.12. Downregulation of the E1 subunit of the PDC protects cells from Ferroptosis. Transient silencing of the E1 subunit of PDC protects cells against erastin induced ferroptosis in the presence of either glucose (A), or pyruvate (B), or DMEM (C). Concentration of glucose or pyruvate were 5.6 mM or 10 mM, respectively. Controls were cells transfected with scrambled nucleotides. Gene (D) and protein expression analysis (E) of control vs silenced cells. Mean ± SD of three independent experiments. Significance calculated by unpaired T test, ****$P < 0.0001$.

In sharp contrast, downregulating the E3 subunit, preventing the enzymatic oxidation of dihydrolipoate, decreased the E_{50} value, either in DMEM (Figure. 13A) or in eDMEM supplemented with glucose or pyruvate (Figure. 13B and 13C). A similar effect was observed with glutamine (Figure. 13D).

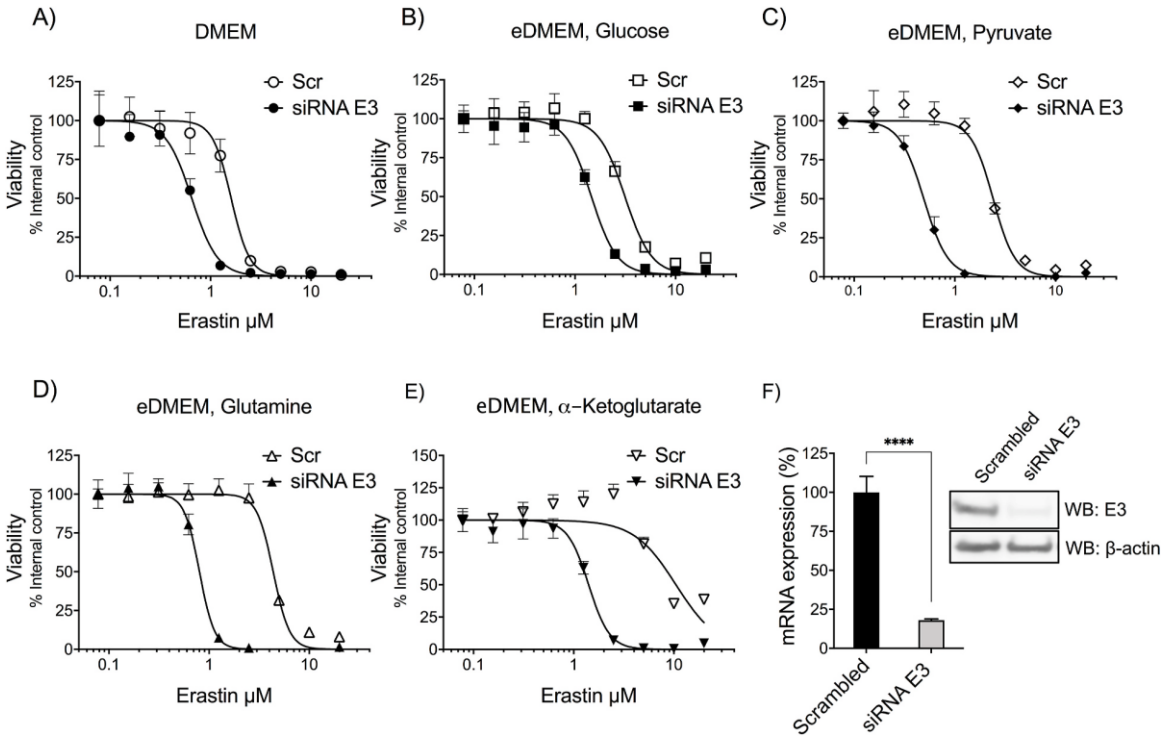

Figure. 13. Downregulation of the E3 subunit of the α-ketoacid dehydrogenase complexes sensitizes cells to Ferroptosis. Transient silencing of the E3 subunit of αKDC sensitizes cells to ferroptosis by erastin in DMEM (A) or in eDMEM containing different substrates (B-D). Concentrations were as follows: 5.6 mM glucose (B); 10 mM pyruvate (C); 4 mM glutamine (D). Controls were cells transfected with scrambled nucleotides. Gene and protein expression analysis (F) of control vs silenced cells. Mean ± SD of three independent experiments. Significance calculated by unpaired T test, ****$P < 0.0001$.

Autoxidation of dihydrolipoate is known producing $O_2^{\bullet-}$ [49-51], therefore, aiming to positively probing the formation of $O_2^{\bullet-}$ in mitochondria, we resorted to use the probe MitoSOX. While conforming this notion we unexpectedly observed that the signal detectable in the presence of pyruvate, was markedly increased by erastin. Oxidation of the probe due to ongoing lipid peroxidation was ruled-out by Fer-1, which does not affect the MitoSOX signal (Figure. 14).

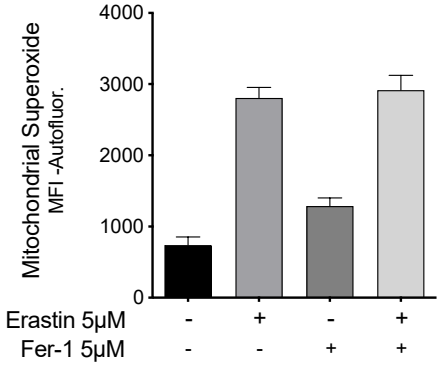

Figure. 14. Erastin promotes $O_2^{\bullet-}$ production in the presence of pyruvate. Cells were incubated in eDMEM containing 10 mM pyruvate for 8 h, where indicated 5 μM erastin was present. Superoxide was detected as MitoSOX fluorescence and was not affected by the ferroptosis inhibitor Fer-1 (5 μM). Mean ± SD of three independent experiments of five replicates for each condition. Significance calculated by ANOVA with Sidak's multiple comparison test, ****$P < 0.0001$.

4.5 Role of Pyruvate Dehydrogenase kinase

This intriguing effect of GSH depletion on superoxide production by the PDC was interpreted in the light of the redox regulation of the PDC inhibitory kinase, pyruvate dehydrogenase kinase (PDK). Being active in the reduced form [52], PDK keeps inhibited the PDC as long as the cellular environment is kept reduced. Consistently, under oxidizing conditions, PDK is inhibited and releases PDC activity. It emerges, therefore, that GSH depletion favours ferroptosis not only by limiting GPx4 activity but, also by activating pyruvate metabolism and the associated production of $O_2^{\bullet-}$.

To verify our hypothesis, we monitored PDK activity, measured by the level of phosphorylation of PDC subunit E1 (phospho-S293).

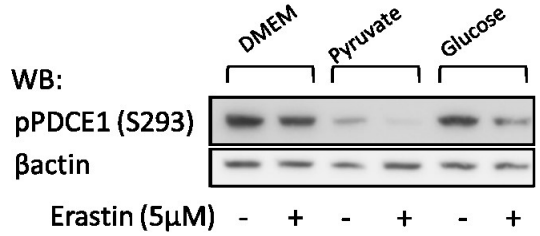

Figure.15. Erastin promotes PDC activation. Cells were plated at a sub-confluent density and 24 hours later DMEM was replaced by eDMEM containing the indicated substrate and erastin or DMEM itself and further incubated for 8 h. Concentrations were as follows: 5.6 mM glucose, 10 mM pyruvate. Cells were lysed and subjected to western blot analysis with specific antibodies.

Erastin decreases pS293 signal, when GSH concentration in the cell falls down. This is indicative of PDK inhibition leading ultimately to PDC activation, fully in agreement with our hypothesis. These results confirm previous findings, suggesting a fine mechanism of PDC control in which the inhibitory kinase associated to the PDC is inhibited by both, an excess of pyruvate and oxidation of the enzyme. This points out the notion that pyruvate feeds forward its own metabolism, which is further stimulated by a decreased nucleophilic tone.

In summary, the more electrophilic environment produced by GSH depletion activates ferroptosis by both priming the formation of lipid hydroperoxides and slowing down GPx4 activity.

4.6 Mechanism of GPx4 inactivation by GSH depletion in HT1080 cells

Accumulating evidences indicate that GSH depletion also activates the autophagic system, with the consequent degradation of ferritin and increase of labile iron pool enhancing the ferroptotic potential [28].

Different studies revealed the crosstalk between autophagy, a conserved intracellular degradation route involved in maintaining cell homeostasis, and ferroptosis [52]. Indeed, lipid peroxidation products (i.e. malondialdehyde [MDA] and 4-hydroxynonenal) are involved in the induction of autophagosome formation. Conversely, over-activation of autophagy seems to be an important driver of ferroptosis. Specifically, certain selective types of autophagy such as ferritinophagy, lipophagy, and chaperone-mediated autophagy [53], facilitate ferroptotic cancer cell death through the degradation of ferroptosis repressors,i.e. ferritin, GPx4, both regulating iron or lipid metabolism.

In this scenario we aimed to gain information on molecular events leading to ferroptosis by using a triterpenoid compound, CDDO, a specific inhibitor of HSP90, which was described to block both necroptosis and ferroptosis. Seemingly, CDDO inhibits GPx4 degradation by blocking chaperone mediated autophagy (CMA) through HSP90 inhibition.

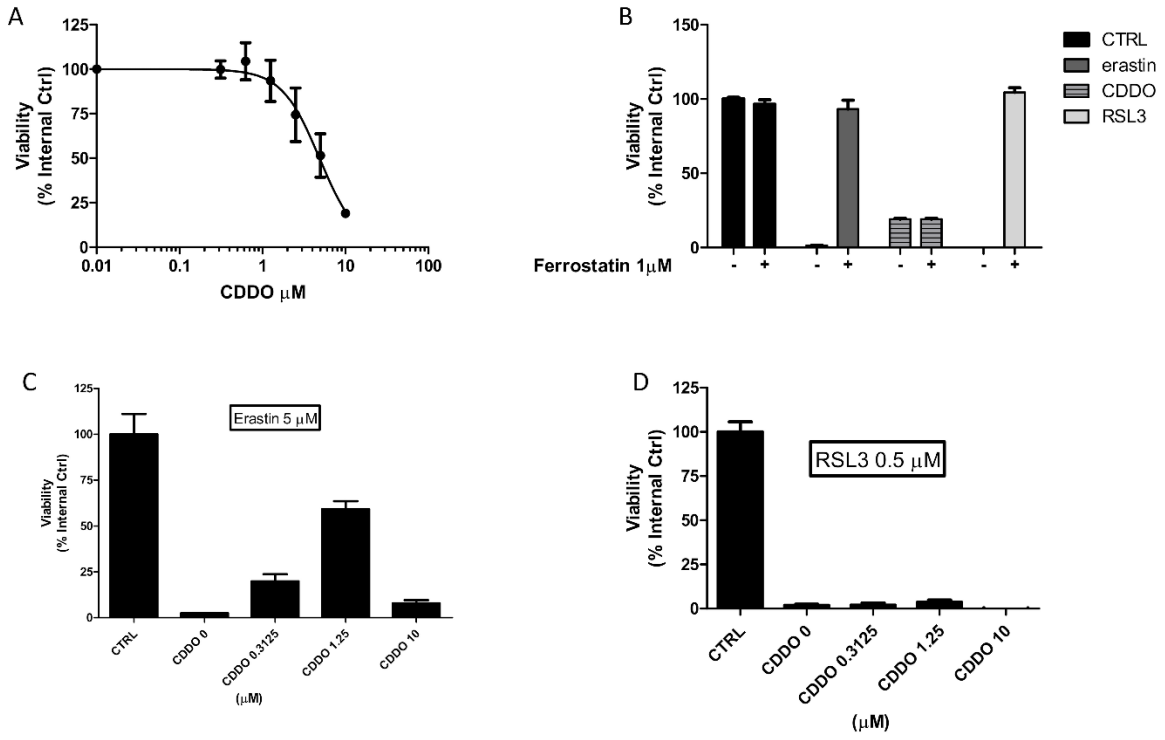

Figure. 16. CDDO protects HT1080 cells to Ferroptosis primed by erastin. Cells were plated at a sub-confluent (5000 cells/ well) density, and the day after DMEM containing erastin or CDDO substituted for DMEM. Incubation further continued 24 h. Cell response to increasing concentrations of CDDO (A), comparison of Fer-1 effects on different treatments (B). Co-treatment of erastin and increasing concentration of CDDO impacts the resistance to ferroptosis. (C). Co-treatment of RSL3 and increasing concentration of CDDO doesn't impact the resistance to ferroptosis. (D). Viability was expressed as % of untreated cells (control). Mean ± SD of three independent experiments of eighteen replicates for each condition. Significance calculated by unpaired T test, $*P < 0.05$.

Preliminary data showed that CDDO clearly induced a non-ferroptotic cell death since Fer-1 couldn't abrogate it (Figure. 16A, 16B column 7 *vs* 6), but it protected cells, although in a narrow concentration range before becoming toxic itself, when ferroptosis was induced by erastin (Figure.16C column 4 *vs* 2). On the other side it was ineffective on ferroptosis due to RSL3 treatment, which directly targets GPx4 enzyme (Figure. 16D). We can infer that the execution of ferroptosis primed by GSH depletion involves, as seen for other cell lines,also the autophagic machinery.

CONCLUSIONS

This study aimed to identify the mechanism of the formation of traces of PL-OOH indispensable to switch on the process of ferroptosis. It is from PL-OOH, indeed, that iron-mediated heterolysis of the O-O bond produces lipid radicals indispensable for the initiation of peroxidative chain reactions. This notion is fundamental for understanding why an efficient GPx4 activity is indispensable to the survival of any aerobically living cell. Differently from other cell death, no specific agonists are required, and ferroptosis only relies on the imbalance between the activity of GPx4 and the continuous formation of PL-OOH that accompanies, in our working hupothesis, aerobic energetic metabolism. It has been known for several decades that oxygen must be activated to react with biological molecules. What intrigued investigators was that lipid peroxidation was not inhibited by scavenging of superoxide or reduction of hydrogen peroxide, while only GPx4 was efficient among enzymatic antioxidant systems. The missing link we propose now is between oxidative metabolism in mitochondria and the formation of a species competent for forming the traces of PL-OOH that GPx4 must continuously reduce to prevent catastrophic oxidative events leading to cell death.

Recent studies pointed out the importance of tricarboxylic acid in ferroptosis primed by GSH depletion.

To investigate the contribution of different metabolic conditions to increase cellular sensitivity to ferroptosis, we set up the experimental model of GSH depletion by erastin in HT1080 cells.

In agreement with previous reports [26,43,48], we obtained clear evidence that the major energetic substrates in the culture medium are indispensable to activation of ferroptosis. The addition of glucose or glutamine to eDMEM, indeed, restored the sensitivity to ferroptosis primed by GSH depletion. Although the pro-ferroptotic effect of both glucose and glutamine had already been observed, our preliminary observations pinpointed more specifically the connection between oxidation of α- ketoacids and sensitivity to ferroptosis. For this reason, we focused on the role of pyruvate, which is the α-ketoacid accounting for the aerobic part of the oxidative metabolism of glucose. First, we found a correlation between pyruvate concentration, lipid peroxidation, and sensitivity to ferroptosis primed by erastin. Second, we focused on the activity of pyruvate dehydrogenase complex. By employing genetic silencing of either the

specific subunit E1 or E3, we provided evidence that $O_2^{\bullet-}$ is generated by dihydrolipoamide reoxidation.

The most reasonable mechanism linking this reaction to lipid peroxidation is the extraction of a methylenic hydrogen of a polyunsaturated fatty acid by the protonated form of superoxide, i.e the hyrdroperoxyl radical ($HO_2^{\bullet}$), which is a powerful oxidant while superoxide anion is not.

Moreover, we observed that the stimulation of $O_2^{\bullet-}$- $HO_2^{\bullet}$ production by pyruvate requires the permissive presence of erastin, hereto pointing out the redox control of the pyruvate metabolism by the PDC. Indeed, available convincing evidence suggests that the inhibitory kinase associated with the PDC is inhibited by both an excess of pyruvate and oxidation of the enzyme [34,26].

In summary, we can infer that aerobic oxidation of pyruvate produces superoxide and that a decreased nucleophilic tone further activates this reaction, in turn allowing a process that, when not inhibited by GPx4, leads to cell death.

Eventually, the decreased nucleophilic tone also accounts for the activation of the autophagic machinery, further facilitating ferroptosis.

In perspective, data obtained in this study indicated that ferroptosis could easily be a physiologically regulated event primed by the coinciding activation of aerobic metabolism of substrates, of which pyruvate is a prototype, with a decreased nucleophilic tone.

From a general point of view, ferroptosis recalls the unique feature of molecular oxygen, which at the same time supports both life and death. Molecular oxygen, indeed, is thermodynamically efficient, although kinetically slow, oxidant [53]. In evolutionary terms, we know that all the species unable to cope with oxygen toxicity died, while the remaining adapted, proliferated, and used oxygen-related radical processes to drive their evolution, integrating the bioenergetic advantage with simultaneous evolution of antioxidant defence [55].

In this scenario lipid peroxidation, which first emerged as one of the major outcomes of oxygen toxicity, is now seen as the executor of a form of regulated cell death encompassing physiological and pathological processes.

REFERENCES

1. Galluzzi L. *et al.* Molecular mechanisms of cell death: recommendations of the Nomenclature Committee on Cell Death 2018. Cell Death Differ. 2018 Mar;25(3):486-541. doi: 10.1038/s41418-017-0012-4..
2. Chen X Li J, Kang R, Klionsky DJ, Tang D. Ferroptosis: machinery and regulation Autophagy. 2020 Aug 26:1-28. doi: 10.1080/15548627.2020.1810918.
3. Galluzzi L, Bravo-San Pedro JM, Kepp O, Kroemer G. Regulated cell death and adaptive stress responses. Cell Mol Life Sci. 2016;73:2405–10. doi: 10.1007/s00018-016-2209-y
4. Dixon SJ, Lemberg KM, Lamprecht MR, Skouta R, Zaitsev EM, Gleason CE, Patel DN, Bauer AJ, Cantley AM, Yang WS, Morrison B 3rd, Stockwell BR. Ferroptosis: An Iron-Dependent Form of Nonapoptotic Cell Death. *Cell* 149, 1060–1072 (2012). doi: 10.1016/j.cell.2012.03.042.
5. Yang WS, SriRamaratnam R, Welsch ME, Shimada K, Skouta R, Viswanathan VS, Cheah JH, Clemons PA, Shamji AF, Clish CB, Brown LM, Girotti AW, Cornish VW, Schreiber SL, Stockwell BR.. Regulation of Ferroptotic Cancer Cell Death by GPX4. *Cell* 156, 317–331 (2014). doi: 10.1016/j.cell.2013.12.010.
6. Hochstein, P. & Ernster, L. Microsomal Peroxidation of Lipids and its Possible Rôle in Cellular Injury. in *Novartis Foundation Symposia* (eds. de Reuck, A. V. S. & Knight, J.) 123–135 (John Wiley & Sons, Ltd., 2008). doi:10.1002/9780470719336.ch7.
7. Jiang X, Stockwell BR, Conrad M. Ferroptosis: mechanisms, biology and role in disease. Nat Rev Mol Cell Biol. 2021 Apr;22(4):266-282. doi: 10.1038/s41580-020-00324-8.
8. Yang W. S. & Stockwell B. R. Synthetic Lethal Screening Identifies Compounds Activating Iron-Dependent, Nonapoptotic Cell Death in Oncogenic-RAS-Harboring Cancer Cells. *Chemistry & Biology* 15, 234–245 (2008). doi: 10.1016/j.chembiol.2008.02.010.
9. Ursini F, Maiorino M & Gregolin C. The selenoenzyme phospholipid hydroperoxide glutathione peroxidase. *Biochimica et Biophysica Acta (BBA) - General Subjects* 839, 62–70 (1985). doi: 10.1016/0304-4165(85)90182-5.
10. Dolma S, Lessnick S L, Hahn WC & Stockwell BR. Identification of genotype-selective antitumor agents using synthetic lethal chemical screening in engineered

human tumor cells. *Cancer Cell* 3, 285–296 (2003). doi: 10.1016/s1535-6108(03)00050-3.

11. Conrad M and Sato H. The oxidative stress-inducible cystine/glutamate antiporter, system x c ⁻: cystine supplier and beyond. Amino Acids 42, 231–246 (2012). doi: 10.1007/s00726-011-0867-5.
12. Bridges RJ, Natale NR and Patel SA. System xc- cystine/glutamate antiporter: an update on molecular pharmacology and roles within the CNS: System xc-cystine/glutamate antiporter. British Journal of Pharmacology 165, 20–34 (2012). doi: 10.1111/j.1476-5381.2011.01480.x.
13. Mandal PK, Seiler A, Perisic T, Kölle P, Banjac Canak A, Förster H, Weiss N, Kremmer E, Lieberman MW, Bannai S, Kuhlencordt P, Sato H, Bornkamm GW, Conrad M. System x c − and Thioredoxin Reductase 1 Cooperatively Rescue Glutathione Deficiency. J. Biol. Chem. 285, 22244–22253 (2010). doi: 10.1074/jbc.M110.121327.
14. Sauzay C, Louandre C, Bodeau S, Anglade F, Godin C, Saidak Z, Fontaine JX, Usureau C, Martin N, Molinie R, Pascal J, Mesnard F, Pluquet O, Galmiche A. Protein biosynthesis, a target of sorafenib, interferes with the unfolded protein response (UPR) and ferroptosis in hepatocellular carcinoma cells. Oncotarget. 2018 Jan 3;9(9):8400-8414. doi: 10.18632/oncotarget.23843.
15. Larraufie MH, Yang WS, Jiang E, Thomas AG, Slusher BS, Stockwell BR.. Incorporation of metabolically stable ketones into a small molecule probe to increase potency and water solubility. Bioorganic & Medicinal Chemistry Letters 25, 4787–4792 (2015). doi: 10.1016/j.bmcl.2015.07.018.
16. Yang WS, Kim KJ, Gaschler MM, Patel M, Shchepinov MS, Stockwell BR. Peroxidation of polyunsaturated fatty acids by lipoxygenases drives ferroptosis. Proc Natl Acad Sci USA 113, E4966–E4975 (2016). doi: 10.1073/pnas.1603244113.
17. Yang, W. S. & Stockwell, B. R. Ferroptosis: Death by Lipid Peroxidation. *Trends in Cell Biology* 26, 165–176 (2016). doi: 10.1016/j.tcb.2015.10.014.
18. Yin H, Xu L, Porter NA.. Free Radical Lipid Peroxidation: Mechanisms and Analysis. *Chem. Rev.* 111, 5944–5972 (2011). doi: 10.1021/cr200084z.
19. Miyamoto S, Martinez GR, Medeiros MH, Di Mascio P. Singlet molecular oxygen generated by biological hydroperoxides, J. Photochem. Photobiol., B 139 (2014) 24–33, doi: 10.1016/j.jphotobiol.2014.03.028.

20. Maiorino M, Conrad M, Ursini F. GPx4, Lipid Peroxidation, and Cell Death: Discoveries, Rediscoveries, and Open Issues. *Antioxidants & Redox Signaling* 29, 61–74 (2018). doi: 10.1089/ars.2017.7115.
21. Dixon SJ, Patel DN, Welsch M, Skouta R, Lee ED, Hayano M, Thomas AG, Gleason CE, Tatonetti NP, Slusher BS, Stockwell BR. Pharmacological inhibition of cystine–glutamate exchange induces endoplasmic reticulum stress and ferroptosis. eLife 3, e02523 (2014). doi: 10.7554/eLife.02523.
22. Dixon SJ, Stockwell BR. The role of iron and reactive oxygen species in cell death. *Nat Chem Biol* 10, 9–17 (2014). doi: 10.1038/nchembio.1416.
23. Seiler A, Schneider M, Förster H, Roth S, Wirth EK, Culmsee C, Plesnila N, Kremmer E, Rådmark O, Wurst W, Bornkamm GW, Schweizer U, Conrad M.Glutathione Peroxidase 4 Senses and Translates Oxidative Stress into 12/15-Lipoxygenase Dependent- and AIF-Mediated Cell Death. *Cell Metabolism* 8, 237–248 (2008). doi: 10.1016/j.cmet.2008.07.005.
24. Doll S, Proneth B, Tyurina YY, Panzilius E, Kobayashi S, Ingold I, Irmler M, Beckers J, Aichler M, Walch A, Prokisch H, Trümbach D, Mao G, Qu F, Bayir H, Füllekrug J, Scheel CH, Wurst W, Schick JA, Kagan VE, Angeli JP, Conrad M. ACSL4 dictates ferroptosis sensitivity by shaping cellular lipid composition. Nat Chem Biol 13, 91–98 (2017). doi: 10.1038/nchembio.2239.
25. Yuan H, Li X, Zhang X, Kang R, Tang D. Identification of ACSL4 as a biomarker and contributor of ferroptosis. Biochemical and Biophysical Research Communications 478, 1338–1343 (2016). doi: 10.1016/j.bbrc.2016.08.124.
26. Gao M, Monian P, Quadri N, Ramasamy R, Jiang X. Glutaminolysis and Transferrin Regulate Ferroptosis. *Molecular Cell* 59, 298–308 (2015). doi: 10.1016/j.molcel.2015.06.011.
27. Andrews NC, Schmidt PJ. Iron Homeostasis. Annu. Rev. Physiol. 69, 69–85 (2007). doi: 10.1146/annurev.physiol.69.031905.164337.
28. Gao M, Monian P, Pan Q, Zhang W, Xiang J, Jiang X. Ferroptosis is an autophagic cell death process. Cell Res 26, 1021–1032 (2016). doi: 10.1038/cr.2016.95.
29. Ursini F, Maiorino M, Valente M, Ferri L, Gregolin C. Purification from pig liver of a protein which protects liposomes and biomembranes from peroxidative degradation and exhibits glutathione peroxidase activity on phosphatidylcholine hydroperoxides. *Biochimica et Biophysica Acta (BBA) - Lipids and Lipid Metabolism* 710, 197–211 (1982). doi: 10.1016/0005-2760(82)90150-3.

30. Flohé L, Loschen G, Günzler WA, Eichele E. Glutathione peroxidase, V. The kinetic mechanism. *Hoppe-Seyler's Z. Physiol. Chem.* 353, 987–999 (1972). doi: 10.1515/bchm2.1972.353.1.987.
31. Gladyshev VN. *et al.* Selenoprotein Gene Nomenclature. *J. Biol. Chem.* 291, 24036–24040 (2016). doi: 10.1074/jbc.M116.756155.
32. Toppo S, Vanin S, Bosello V, Tosatto SC. Evolutionary and Structural Insights Into the Multifaceted Glutathione Peroxidase (Gpx) Superfamily. *Antioxidants & Redox Signaling* 10, 1501–1514 (2008). doi: 10.1089/ars.2008.2057.
33. Brigelius-Flohé R, Maiorino M. Glutathione peroxidases. *Biochimica et Biophysica Acta (BBA) - General Subjects* 1830, 3289–3303 (2013). doi: 10.1016/j.bbagen.2012.11.020
34. Toppo S, Flohé L, Ursini F, Vanin S, Maiorino M. Catalytic mechanisms and specificities of glutathione peroxidases: Variations of a basic scheme. *Biochimica et Biophysica Acta (BBA) - General Subjects* 1790, 1486–1500 (2009). doi: 10.1016/j.bbagen.2009.04.007
35. Orian L, Mauri P, Roveri A, Toppo S, Benazzi L, Bosello-Travain V, De Palma A, Maiorino M, Miotto G, Zaccarin M, Polimeno A, Flohé L, Ursini F. Selenocysteine oxidation in glutathione peroxidase catalysis: an MS-supported quantum mechanics study. *Free Radical Biology and Medicine* 87, 1–14 (2015). doi: 10.1016/j.freeradbiomed.2015.06.011.
36. Ingold I, Berndt C, Schmitt S, Doll S, Poschmann G, Buday K, Roveri A, Peng X, Porto Freitas F, Seibt T, Mehr L, Aichler M, Walch A, Lamp D, Jastroch M, Miyamoto S, Wurst W, Ursini F, Arnér ESJ, Fradejas-Villar N, Schweizer U, Zischka H, Friedmann Angeli JP, Conrad M.. Selenium Utilization by GPX4 Is Required to Prevent Hydroperoxide-Induced Ferroptosis. *Cell* 172, 409-422.e21 (2018). doi: 10.1016/j.cell.2017.11.048.
37. Shi ZZ, Osei-Frimpong J, Kala G, Kala SV, Barrios RJ, Habib GM, Lukin DJ, Danney CM, Matzuk MM, Lieberman MW. Glutathione synthesis is essential for mouse development but not for cell growth in culture. *Proceedings of the National Academy of Sciences* 97, 5101–5106 (2000). doi: 10.1073/pnas.97.10.5101.
38. Hayano, M., Yang, W. S., Corn, C. K., Pagano, N. C. & Stockwell, B. R. Loss of cysteinyl-tRNA synthetase (CARS) induces the transsulfuration pathway and inhibits ferroptosis induced by cystine deprivation. *Cell Death Differ* 23, 270–278 (2016).

39. Erickson AM, Nevarea Z, Gipp JJ, Mulcahy RT. Identification of a Variant Antioxidant Response Element in the Promoter of the Human Glutamate-Cysteine Ligase Modifier Subunit Gene: revision of the ARE consensus sequence. *J. Biol. Chem.* 277, 30730–30737 (2002). doi: 10.1074/jbc.M205225200.
40. Ursini F, Maiorino M. Lipid peroxidation and ferroptosis: The role of GSH and GPx4. Free Radic Biol Med. 2020 May 20;152:175-185. doi: 10.1016/j.freeradbiomed.2020.02.027.
41. Doll S, et al. FSP1 is a glutathione-independent ferroptosis suppressor. Nature 2019, 575, 693–698. doi: 10.1038/s41586-019-1707-0
42. Bersuker K, Hendricks JM, Li Z, Magtanong L, Ford B, Tang PH, Roberts MA, Tong B, Maimone TJ, Zoncu R, Bassik MC, Nomura DK, Dixon SJ, Olzmann JA. The CoQ oxidoreductase FSP1 acts parallel to GPX4 to inhibit ferroptosis. Nature 2019, 575, 688–692. doi: 10.1038/s41586-019-1705-2
43. Gao M, Yi J, Zhu J, Minikes AM, Monian P, Thompson CB, Jiang X. Role of Mitochondria in Ferroptosis. Mol Cell, 73 (2) (2019), pp. 354-363, doi: 10.1016/j.molcel.2018.10.042.
44. Stockwell BR, et al. Ferroptosis: A Regulated Cell Death Nexus Linking Metabolism, Redox Biology, and Disease. Cell. 2017 Oct 5;171(2):273-285. doi: 10.1016/j.cell.2017.09.021.
45. Tietze F. Enzymic method for quantitative determination of nanogram amounts of total and oxidized glutathione: applications to mammalian blood and other tissues, Anal. Biochem. 27 (3) (1969) 502–522. doi: 10.1016/0003-2697(69)90064-5.
46. Gao M, Jiang X. To eat or not to eat-the metabolic flavor of ferroptosis, Curr. Opin. Cell Biol. 51 (2018) 58–64. doi: 10.1016/j.ceb.2017.11.001.
47. Vučković AM, Bosello Travain V, Bordin L, Cozza G, Miotto G, Rossetto M, Toppo S, Venerando R, Zaccarin M, Maiorino M, Ursini F, Roveri A. Inactivation of the glutathione peroxidase GPx4 by the ferroptosis-inducing molecule RSL3 requires the adaptor protein 14-3-3ε. FEBS Lett. 2020 Feb;594(4):611-624. doi: 10.1002/1873-3468.13631.
48. Quinlan CL, Goncalves RL, Hey-Mogensen M, Yadava N, Bunik VI, Brand MD. The 2-oxoacid dehydrogenase complexes in mitochondria can produce superoxide/hydrogen peroxide at much higher rates than complex I. J. Biol. Chem., 289 (12) (2014), pp. 8312-8325,10.1074/jbc.M113.545301

49. Bunik VI, Brand MD. Generation of superoxide and hydrogen peroxide by side reactions of mitochondrial 2-oxoacid dehydrogenase complexes in isolation and in cells. Biol. Chem. 399 (5) (2018) 407–420. doi: 10.1515/hsz-2017-0284.
50. Bunik V.I. Redox-Driven Signaling: 2-Oxo Acid Dehydrogenase Complexes as Sensors and Transmitters of Metabolic Imbalance. Antioxidants Redox Signal. 30 (16) (2019) 1911–1947. doi: 10.1089/ars.2017.7311.
51. Hurd TR, Collins Y, Abakumova I, Chouchani ET, Baranowski B, Fearnley IM, Prime TA, Murphy MP, James AM. Inactivation of pyruvate dehydrogenase kinase 2 by mitochondrial reactive oxygen species. J. Biol. Chem. 287 (42) (2012) 35153–35160. doi: 10.1074/jbc.M112.400002.
52. Li J, et al. Autophagy. 2021 Jan 15:1-14. doi: 1a0.1080/15548627.2021.1872241.
53. Wu Z, Geng Y, Lu X, Shi Y, Wu G, Zhang M, Shan B, Pan H, Yuan J. Chaperone-mediated autophagy is involved in the execution of ferroptosis. Proc Natl Acad Sci U S A. 2019 Feb 19;116(8):2996-3005. doi: 10.1073/pnas.1819728116.
54. Ernster L, Oxygen as an environmental poison, Chem. Scripta 26 (4) (1986):525–534
55. Gutteridge JMC, Halliwell B. Mini-Review: oxidative stress, redox stress or redox success? Biochem. Biophys. Res. Commun. 502 (2) (2018) 183–186. doi: 10.1016/j.bbrc.2018.05.045.